View metadata, citation and similar papers at core.ac.uk

brought to you by CORE

provided by IntechOpen

We are IntechOpen, the world's leading publisher of Open Access books Built by scientists, for scientists

4,800
Open access books available

122,000
International authors and editors

135M
Downloads

Our authors are among the

154
Countries delivered to

TOP 1%
most cited scientists

12.2%
Contributors from top 500 universities

CLARIVATE ANALYTICS BOOK CITATION INDEX INDEXED

WEB OF SCIENCE™

Selection of our books indexed in the Book Citation Index in Web of Science™ Core Collection (BKCI)

Interested in publishing with us?
Contact book.department@intechopen.com

Numbers displayed above are based on latest data collected.
For more information visit www.intechopen.com

23

Thermodynamics and Thermokinetics to Model Phase Transitions of Polymers over Extended Temperature and Pressure Ranges Under Various Hydrostatic Fluids

Séverine A.E. Boyer[1], Jean-Pierre E. Grolier[2],
Hirohisa Yoshida[3], Jean-Marc Haudin[4] and Jean-Loup Chenot[4]
[1]*Institut P PRIME-P', ISAE-ENSMA, UPR CNRS 3346, Futuroscope Chasseneuil*
[2]*Université Blaise Pascal de Clermont-Ferrand, Laboratoire de Thermodynamique, UMR CNRS 6272, Aubière*
[3]*Tokyo Metropolitan University, Faculty of Urban Environmental Science, Tokyo*
[4]*MINES ParisTech, CEMEF, UMR CNRS 7635, Sophia Antipolis*
[1,2,4]*France*
[3]*Japan*

1. Introduction

A scientific understanding of the behaviour of polymers under extreme conditions of temperature and pressure becomes inevitably of the utmost importance when the objective is to produce materials with well-defined final in-use properties and to prevent the damage of materials during on-duty conditions. The proper properties as well as the observed damages are related to the phase transitions together with intimate pattern organization of the materials.

Thermodynamic and thermokinetic issues directly result from the thermodynamic independent variables as temperature, pressure and volume that can stay constant or be scanned as a function of time. Concomitantly, these variables can be coupled with a mechanical stress, the diffusion of a solvent, and/or a chemically reactive environment. A mechanical stress can be illustrated in a chemically inert environment by an elongation and/or a shear. Diffusion is typically described by the sorption of a solvent. A chemical environment is illustrated by the presence of a reactive environment as carbon dioxide or hydrogen for example.

Challenging aspects are polymer pattern multi scale organizations, from the nanometric to the macrometric scale, and their importance regarding industrial and technological problems, as described in the state of the art in Part 2. New horizons and opportunities are at hands through pertinent approaches, including advanced *ad hoc* experimental techniques with improved modelling and simulation. Four striking illustrations, from the interactions between a solvent and a polymer to the growth patterns, are illustrated in Part 3.

2. Multi-length scale pattern formation with *in-situ* advanced techniques

2.1 Structure formation in various materials

2.1.1 Broad multi-length scale organization

The development of polymer-type patterns is richly illustrated in the case of biological materials and metals.

Pattern growth

Among the observed morphologies which extend from polymeric to metallic materials and to biologic species, similar pattern growth is observed. Patterns extend, with a multilevel branching, from the nanometric **(Fig. 1.a-b)** to the micrometric **(Fig. 1.c-d-e)** scale structures.

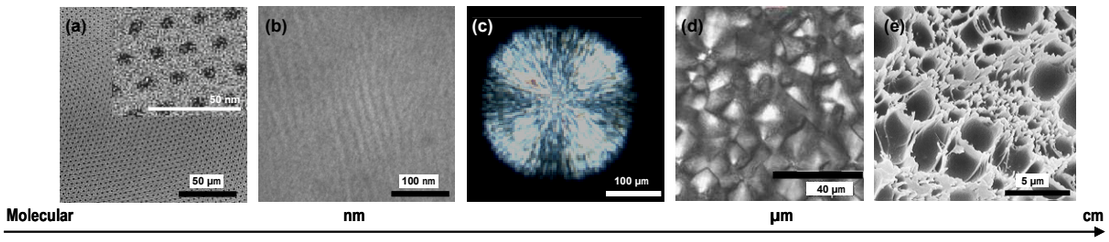

Fig. 1. Two-dimensional (2D) observations of various polymer patterns. **(a)** nanometric scale pattern of poly(ethylene-oxide) cylinders (PEO in black dots) in amphiphilic diblock copolymer PEO_m-*b*-$PMA(Az)_n$ (**a**, Iwamoto & Boyer, CREST-JSPS, Tokyo, Japan), **(b)** nanometric scale lamellae of an isotactic polypropylene (iPP, crystallization at 0.1 °C.min^{-1}, $RuCl_3$ stained) with crystalline lamella thickness of 10 nm in order of magnitude, **(c)** micrometric scale of an iPP spherulite with lamellar crystals radiating from a nucleating point (iPP, crystallization at 140 °C), **(d)** micrometric scale structure of a polyether block amide after injection moulding (**b-c-d**, Boyer, CARNOT-MINES-CEMEF, Sophia Antipolis, France), **(e)** micrometric scale cellular structure of a polystyrene damaged under carbon dioxide sorption at 317 K (**e**, Hilic & Boyer, Brite Euram POLYFOAM Project BE-4154, Clermont-Ferrand, France).

The polycrystalline features, formed by freezing an undercooled melt, are governed by dynamical processes of growth that depend on the material nature and on the thermodynamic environment. Beautiful illustrations are available in the literature. To cite a few, the rod-like eutectic structure is observed in a dual-phase pattern, namely for metallic with ceramic, and for polymeric (De Rosa et al., 2000; Park et al., 2003) systems like nanometric length scale of hexagonal structure of poly(ethylene-oxide) PEO cylinders in amphiphilic diblock copolymer PEO_m-*b*-$PMA(Az)_n$ with azobenzene part PMA(Az) (Tian et al., 2002). Dendritic patterns are embellished with images like snowflake ice dendrites from undercooled water (Kobayashi, 1993) and primary solidified phase in most metallic alloys (*e.g.*, steel, industrial alloys) (Trivedi & Laorchan, 1988a-b), and even dendrites in polymer blends (Ferreiro et al., 2002a) like PEO polymer dendrites formed under cooling PEO/polymethyl methacrylate PMMA blend (Gránásy et al., 2003; Okerberg et al., 2008). In the nanometric scale, immiscibility of polymer chains in block copolymers leads to microphase-separated structures with typical morphologies like hexagonally packed cylindrical structures, lamellae, spheres in centred cubic phases, double gyroid and double diamond networks (Park et al., 2003).

In polymer physics, the spherulitic crystallization **(Fig. 1.c)** represents a classic example of pattern formation. It is one of the most illustrated in the literature. Besides their importance in technical polymers, spherulitic patterns are also interesting from a biological point of view like semicrystalline amyloid spherulites associated with the Alzheimer and Kreutzfeld-Jacob diseases (Jin et al., 2003; Krebs et al., 2005). The spherulitic pattern depends on polymer chemistry (Ferreiro et al., 2002b). Stereo irregular atactic or low molecular weight compounds are considered as impurities, which are rejected by growing crystals. The openness of structure, from spherulite-like to dendrite-like, together with the coarseness of texture (a measure of the 'diameters' of crystalline fibres between which impurities become concentrated during crystal growth) was illustrated in the work of Keith & Padden (1964). These processes induce thermal and solute transport. Thus pattern formation is defined by the dynamics of the crystal/melt interface involving the interfacial energy. In the nanometric scale domain, spherulite is a cluster of locally periodic arrays of crystalline layers distributed as radial stacks of parallel crystalline lamellae separated by amorphous layers **(Fig. 1.b)**. Molecular chains through the inter-lamellar amorphous layers act as tie molecules between crystalline layers, making a confined interphase crystalline lamellae/amorphous layer.

Cross fertilization between polymer crystallization and metal solidification

Physical chemists and metallurgists alike are constantly confronted with materials properties related to (polymer) crystallization (*e.g.*, spherulite size distribution, lamellae spacing) or (metal) solidification (*e.g.*, grain size distribution, dendrite arm or eutectic spacing), respectively. In metal science, if accurate numerical modelling of dendritic growth remains a major challenge even with today's powerful computers, the growth kinetic theories, using accurate surface tension and/or kinetic anisotropies, are well advanced (Asta et al., 2009; Flemings, 1974). In polymer science, such approaches exist. But still insight into the physics/kinetics connection and morphologies is little known (Piorkowska et al., 2006). The most well-known growth kinetics theory is the one of Hoffman and coworkers (Hoffman, 1983) which is based on the concept of secondary nucleation; the nucleation and overall kinetics of crystallization have been also intensively studied (Avrami, 1939, 1940, 1941; Binsbergen, 1973; Haudin & Chenot, 2004).

2.1.2 Practical applications, importance of crystal organization

The multi-length scale and semi-crystalline structure organizations are intimately linked with the chemical, physical, mechanical integrity and failure characteristics of the materials.

Polymers with well-defined end-used properties

Semi-crystalline polymers gain increasing importance in manufacturing (extended to recycling) industries where the control at the nano- to micro- up to macrometric hierarchical levels of the patterns constitutes a major engineering challenge (Lo et al., 2007). The domains extend from optics, electronics, magnetic storage, isolation to biosorption, medicine, packaging, membranes and even food industry (Rousset et al., 1998; Winter et al., 2002; Park et al., 2003; Nowacki et al., 2004; Scheichl et al., 2005; Sánchez et al., 2007; Wang et al., 2010).

Control of polymer structure in processing conditions

Industrial polymer activities, through processes like, for instance, extrusion coating (*i.e.*, the food industry with consumption products), injection moulding (*i.e.*, the industry with

engineering parts for automotive or medicine needs) (Devisme et al., 2007; Haudin et al., 2008), deal with polymer formulation and transformation. The viscous polymer melt partially crystallizes after undergoing a complex flow history or during flow, under temperature gradients and imposed pressure (Watanabe et al., 2003; Elmoumni & Winter, 2006) resulting into a non homogeneous final macrometric structure throughout the thickness of the processed part. The final morphologies are various sizes and shapes of more or less deformed spherulites resulting from several origins: *i)* isotropic spherulites by static crystallization (Ferreiro et al., 2002a; Nowacki et al., 2004), *ii)* highly anisotropic morphologies as oriented and row-nucleated structures (*i.e.*, shish-kebabs) by specific shear stress (Janeschitz-Kriegl, 2006; Ogino et al., 2006), *iii)* transcrystalline layer (as columnar pattern in metallurgy) by surface nucleation and/or temperature gradient, and *iv)* teardrop--shaped spherulites or "comets" (spherulites with a quasi-parabolic outline) by temperature gradients (Ratajski & Janeschitz-Kriegl, 1996; Pawlak et al., 2002).

Together with the deformation path (*e.g.*, tension, compression), the morphology strongly influences the behaviour of polymers. Some models have attempted to predict the properties of spherulites through a simulation of random distributions of flat ellipsoids (crystalline lamellae) embedded in an amorphous phase described by a finite extensible rubber network (Ahzi et al., 1991; Dahoun et al., 1991; Arruda & Boyce, 1993; Bedoui et al., 2006).

Moreover by considering the high-pressure technology, the use of specific fluids plays a non negligible role in pattern control. The thermodynamic phase diagrams of fluids implies the three coordinates (pressure-volume-temperature, *PVT*, variables) representation where the fluids can be in the solid, gaseous, liquid and even supercritical state. The so-called "signature of life" water (H_2O) (Glasser, 2004) and the so-called "green solvent" in fact "clean safe" carbon dioxide (CO_2) (Glasser, 2002) can be cited. The use of H_2O is encountered in injection moulding assisted with water. CO_2 is known as a valuable agent in polymer processing thanks to its aptitude to solubilize, to plasticize (Boyer & Grolier, 2005), to reduce viscosity, to favour polymer blending or to polymerize (Varma-Nair et al., 2003; Nalawade et al., 2006). In polymer foaming, elevated temperatures and pressures are involved as well as the addition of chemicals, mostly penetrating agents that act as blowing agents (Tomasko et al., 2003; Lee et al., 2005).

Damage of polymer structure in on-duty conditions

In the transport of fluids, in particular in the petroleum industry taken as an example, flexible hosepipes are used which engineering structures contain extruded thermoplastic or rubber sheaths together with reinforcing metallic armour layers. Transported fluids contain important amounts of dissolved species, which on operating temperature and pressure may influence the resistance of the engineering structures depending on the thermodynamic *T*, *P*-conditions and various phenomena as sorption/diffusion, chemical interactions (reactive fluids, *i.e.*, oxidation), mechanical (confinement) changes. The polymer damage occurs when rupture of the thermodynamic equilibrium (*i.e.*, after a sharp pressure drop) activates the blistering phenomenon, usually termed as 'explosive decompression failure' (XDF) process (Dewimille et al., 1993; Rambert et al., 2006; Boyer et al., 2007; Baudet et al., 2009). Damage is a direct result of specific interactions between semi-crystalline patterns and solvent with a preferential interaction (but not exclusive) in the amorphous phase (Klopffer & Flaconnèche, 2001).

2.2 Development of combined experimental procedures

The coupling of thermodynamic and kinetic effects (*i.e.*, confinement, shear flow, thermal gradient) with diffusion (*i.e.*, pressurizing sorption,) and chemical environment *(i.e.*, polar effect, oxidation), and the consideration of the nature of the polymers *(i.e.*, homopolymers, copolymers, etc.) require a broad range of indispensable *in-situ* investigations. They aim at providing well-documented thermodynamic properties and phase transitions profiles of polymers under various, coupled and extreme conditions.

2.2.1 Temperature control at atmospheric pressure

Usual developed devices are based on the control of temperature, while the main concerns are high cooling rate control and shearing rate.

The kinetic data of polymer crystallization are often determined in isothermal conditions or at moderate cooling rates. The expressions are frequently interpreted using simplified forms of Avrami's theory involving thus Avrami's exponent and a temperature function, which can be derived from Hoffman-Lauritzen's equation **(**Devisme et al., 2007). However, such an interpretation cannot be extrapolated to low crystallization temperatures encountered in polymer processing, *i.e.*, to high cooling rates (Magill, 1961, 1962, 2001; Haudin et al., 2008; Boyer et al., 2011b). In front of the necessity for obtaining crystallization data at high cooling rates, different technical solutions are proposed. Specific hot stages (Ding & Spruiell, 1996; Boyer & Haudin, 2010), quenching of thin polymer films (Brucato et al., 2002), and nanocalorimetry (Schick, 2009) are the main designs.

Similarly, to generate a controlled melt shearing, various shearing devices have been proposed, for instance, home-made sliding plate (Haudin et al., 2008) and rotating parallel plate devices (*e.g.*, Linkam temperature controlled stage, Haake Mars modular advanced rheometer system). The shear-induced crystallization can be performed according to a 'long' shearing protocol as compared to the 'short-term' shearing protocol proposed by the group of Janeschitz-Kriegl (Janeschitz-Kriegl et al., 2003, 2006; Baert et al., 2006).

2.2.2 Temperature-pressure-volume control

The design of devices based on the control of pressure requires breakthrough technologies. The major difficulty is to generate high pressure.

In polymer solidification, the effects of pressure can be studied through pressure–volume–temperature phase diagrams obtained during cooling at constant pressure. The effect of hydrostatic (or inert) pressure on phase transitions is to shift the equilibrium temperature to higher values, *e.g.*, the isotropic phase changes of complex compounds as illustrated in the works of Maeda et al. (2005) by high-pressure differential thermal analyzer and of Boyer et al. (2006a) by high-pressure scanning transitiometry, or the melting temperature in polymer crystallization as illustrated for polypropylene in the work of Fulchiron et al. (2001) by high-pressure dilatometry. However, classical dilatometers cannot be operated at high cooling rate without preventing the occurrence of a thermal gradient within the sample. This problem can be solved by modelling the dilatometry experiment (Fulchiron et al., 2001) or by using a miniaturized dilatometer (Van der Beek et al., 2005). Alternatively, other promising technological developments propose to couple the pressure and cooling rates as shown with an apparatus for solidification based on the confining fluid technique as described by Sorrentino et al. (2005). The coupling of pressure and shear is possible with the shear flow pressure–volume–temperature measurement system developed by Watanabe et

al. (2003). Presently, performing of *in-situ* observations of phase changes based on the optical properties of polymers (Magill, 1961, 2001) under pressure is the object of a research project developed by Boyer (Boyer et al., 2011a).
To estimate the solubility of penetrating agents in polymers, four main approaches are currently generating various techniques and methods, namely: gravimetric techniques, oscillating techniques, pressure decay methods, and flow methods. However, with many existing experimental devices, the gain in weight of the polymer is measured whereas the associated volume change is either estimated or sometimes neglected (Hilic et al., 2000; Nalawade et al., 2006; Li et al., 2008).
The determination of key thermo-mechanical parameters coupled with diffusion and chemical effects together with temperature and pressure control is not yet well established. Approaches addressing the prediction of the multifaceted thermo-diffuso-chemo-mechanical (TDCM) behaviour are being suggested. Constitutive equations are built within a thermomechanical framework, like the relation based on a rigorous thermodynamic approach (Boyer et al., 2007), and the proposed formalism based on as well rigorous mechanical approach (Rambert et al., 2006; Baudet et al., 2009).

3. Development and optimization of pertinent models

Modelling of polymer phase transitions with a specific thermodynamics- and thermokinetics-based approach assumes to consider the coupling between thermal, diffusion, chemical and mechanical phenomena and to develop advanced physically-based polymer laws taking into account the morphologies and associated growth. This implies a twofold decisive step, theoretical and experimental.
As regards specific industrial and technological problems, from polymer formulation to polymer damage, passing by polymer processing, the conceptualization involves largely different size scales with extensive and smart experimentation to suggest and justify suitable approximations for theoretical analyses.

3.1 Thermodynamics as a means to understand and prevent macro-scale changes and damages resulting from molten or solid polymer/solvent interactions

Thermodynamics is a useful and powerful means to understand and prevent polymer macro-scale changes and damages resulting from molten or solid material/solvent interactions. Two engineering examples are illustrative: foaming processes with hydrochlorofluorocarbons (HCFCs) as blowing agents in extrusion processes with a concern on safeguarding the ozone layer and the global climate system, Montreal Protocol (Dixon, 2011), and transport of petroleum fluids with in-service pipelines made of structural semi-crystalline polymers which are then exposed to explosive fluctuating fluid pressure (Dewimille et al., 1993).

Solubility and concomitant swelling of solvent-saturated molten polymer

In the prediction of the relevant thermo-diffuso-chemo-mechanical behaviour of polymers, sorption is the central phenomenon. Sorption is by nature complex, since the effects of fluids solubility in polymers and of the concomitant swelling of these polymers cannot be separated.
To experimentally extract reliable solubility data, the development of inventive equipments is required. In an original way, dynamic pendulum technology under pressure is used. The advanced development proposes to combine the features of the vibrating-wire viscometer

with a high pressure decay technique, the whole setup being operated under a fine control of the temperature. The limits and performances of this mechanical setup under extreme conditions, *i.e.*, pressure and environment of fluid, were theoretically assessed (Boyer et al., 2007). In the working equation of the vibrating-wire sensor (VW) **(eq. (1))**, unknowns are both the mass m_{sol} of solvent absorbed in the polymer and the associated change in volume ΔV_{pol} of the polymer due to the sorption.

$$m_{sol} = \rho_g \, \Delta V_{pol} + \left[\left(\omega_B^2 - \omega_0^2 \right) \frac{4 \, L^2 \, R^2 \, \rho_S}{\pi \, g} + \rho_g \left(V_C + V_{pol} \right) \right] \tag{1}$$

The volume of the degassed polymer is represented by V_{pol} and ρ_g is the density of the solvent. The other parameters are the physical characteristics of the wire, namely, ω_0 and ω_B which represent the natural (angular) frequencies of the wire in vacuum and under pressure, respectively. And L, R, ρ_s are, respectively, the length, the radius and the density of the wire. V_C is the volume of the polymer container.

The thermodynamics of solvent-polymer interactions can be theoretically expressed with a small number of adjustable parameters. The currently used models are the 'dual-mode' model (Vieth et al., 1976), the cubic equation of state (EOS) as Peng-Robinson (Zhong & Masuoka, 1998) or Soave-Redlich-Kwong (Orbey et al., 1998) EOSs, the lattice-fluid model of Sanchez–Lacombe equation of state (SL-EOS) (Lacombe & Sanchez, 1976; Sanchez & Lacombe, 1976) with the extended equation of Doghieri-Sarti (Doghieri & Sarti, 1996; Sarti & Doghieri, 1998), and the Statistical Associating Fluid Theory (SAFT) (Prigogine et al., 1957; Beret & Prausnitz, 1975; Behme et al., 1999).

From the state of the art, the thermodynamic SL-EOS was preferably selected to theoretically estimate the change in volume of the polymer *versus* pressures and temperatures found in **eq. (1)**. In this model, phase equilibria of pure components or solutions are determined by equating chemical potentials of a component in coexisting phases. It is based on a well-defined statistical mechanical model, which extends the basic Flory-Huggins theory (Panayiotou & Sanchez, 1991). Only one binary adjustable interaction parameter k_{12} has to be calculated by fitting the sorption data **eqs. (2-4)**. In the mixing rule appears the volume fraction of the solvent (index $_1$, ϕ_1) in the polymer (index $_2$, ϕ_2), (ρ_1^* , p_1^* , T_1^*) and (ρ_2^* , p_2^* , T_2^*) being the characteristic parameters of pure compounds.

$$p^* = \phi_1 p_1^* + \phi_2 p_2^* - \phi_1 \phi_2 \Delta p^* \tag{2}$$

$$T^* = \frac{p^*}{\dfrac{\phi_1 \; p_1^*}{T_1^*} + \dfrac{\phi_2 p_2^*}{T_2^*}} \tag{3}$$

The parameter Δp^* characterizes the interactions in the mixture. It is correlated with the binary adjustable parameter k_{12}.

$$\Delta p^* = k_{12} \sqrt{p_1^* \, p_2^*} \tag{4}$$

The mass fraction of solvent (the permeant), ω_1, at the thermodynamical equilibrium is calculated with **eq. (5)**.

$$\omega_1 = \frac{\phi_1}{\phi_1 + \left(1 - \phi_1\right)\frac{\rho_2^*}{\rho_1^*}} \tag{5}$$

Coupled with the equation of DeAngelis (DeAngelis et al., 1999), the change in volume ΔV_{pol} of the polymer is accessible via **eq. (6)**:

$$\frac{\Delta V_{pol}}{V_0} = \frac{1}{\tilde{\rho}\rho^*\left(1 - \omega_1\right)}\frac{1}{\hat{\upsilon}_2^0} \tag{6}$$

ρ^* and $\tilde{\rho}$ are the mixture characteristic and reduced densities, respectively. $\hat{\upsilon}_2^0$ is the specific volume of the pure polymer at fixed *T*, *P* and composition. The correlation with the model is done in conjunction with the optimization of the parameter k_{12} that minimizes the *A*verage of *A*bsolute *D*eviations (*AAD*) between the experimental results and the results recalculated from the fit.

The critical comparison between the semi-experimental (or semi-theoretical) data of solubility and pure-experimental data available in the literature allows us to validate the consistency of the methodology of the calculations. The combination of coupled experimental and calculated data obtained from the vibrating-wire and theoretical analyses gives access to original solubility data that were not up to now available for high pressure in the literature. As an illustration in **Fig. 2.a-b** is given the solubility of carbon dioxide (CO_2) and of 1,1,1,2-tetrafluoroethane (HFC-134a) in molten polystyrene (PS). HFC-134a is significantly more soluble in PS by a factor of two compared to CO_2. The parameter k_{12} was estimated at 0.9232, 0.9342, 0.9140 and 0.9120 for CO_2 sorption respectively at 338, 362, 383 and 402 K. For HFC-134a sorption, it was estimated at 0.9897 and 0.9912 at 385 and 402 K, respectively. The maximum of the polymer volume change was in CO_2 of 13 % at 25 MPa and 338 K, 15 % at 25 MPa and 363 K, 14 % at 43 MPa and 383 K, 13 % at 44 MPa and 403 K, and in HFC-134a of 12 % at 16 MPa and 385K, 11 % at 20 MPa and 403 K. thermodynamic behaviour of {PS-permeant} systems with temperature is comparable to a lower critical solution temperature (LCST) behaviour (Sanchez & Lacombe, 1976).

From these data, the aptitude of the thermodynamic SAFT EOS to predict the solubility of carbon dioxide and of 1,1,1,2-tetrafluoroethane (HFC-134a) in polystyrene (PS) is evaluated. The use of SAF theoretical model is rather delicate because the approach uses a reference fluid that incorporates both chain length (molecular size and shape) and molecular association. SAF Theory is then defined in terms of the residual Helmholtz energy a^{res} per mole. And a^{res} is represented by a sum of three intermolecular interactions, namely, segment–segment interactions, covalent chain-forming bonds among segments and site-site interactions such as hydrogen bond association. The SAFT equation satisfactorily applies for CO_2 dissolved in PS with a molecular mass in weight near about 1000 g.mol^{-1}, while it is extended to HFC-134a dissolved in PS with a low molecular mass in weight.

Global cubic expansion coefficient of solvent saturated polymer as thermo-diffuso-chemo-mechanical parameter for preferential control of solid polymer/solvent interactions

An essential additional information to solubility quantification, in direct relation with polymer damage by dissolved gases, is the expansion coefficient of the gas saturated polymer, *i.e.*, the mechanical cubic expansion coefficient of the polymer saturated in a solvent, $\alpha_{pol\text{-}g\text{-}int}$.

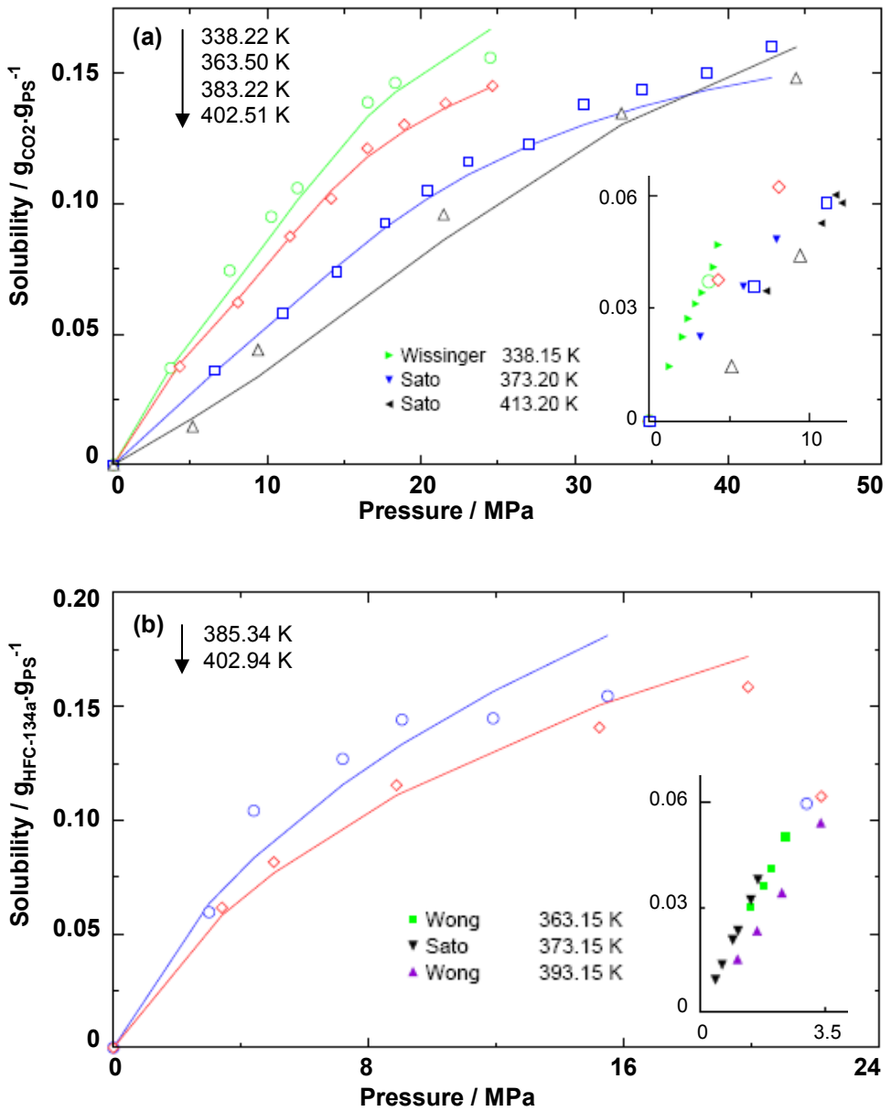

Fig. 2. Solubility of **(a)** CO_2 (critical pressure (P_c) of 7.375 MPa, critical temperature (T_c) of 304.13 K) and **(b)** HFC-134a (P_c of 4.056 MPa, T_c of 374.18 K) in PS with **(a-insert)** literature data from pressure decay measurement (Sato et al., 1996, pressure up to 20 MPa), from elongation measurement (Wissinger & Paulaitis, 1987, pressure up to 5 MPa**),** and **(b-insert)** literature data from volumetric measurement (Sato et al., 2000, pressure up to 3 MPa), from gravimetry (Wong et al., 1998, pressure up to 4 MPa**)**. The correlation of CO_2 and HFC-134a solubility in PS with SAFT is illustrated with solid lines.

A precise experimental methodology and a mathematical development proposed by Boyer (Boyer et al., 2006b, 2007) use the thermodynamic approach of high-pressure-controlled scanning transitiometry (*P*CST) (Grolier et al., 2004; Bessières et al., 2005). The heat resulting from the polymer/solvent interactions is measured during pressurization/depressurization runs performed under isothermal scans. Several binary polymer/fluid systems with a more or less reactive pressurizing medium have been investigated with a view to illustrate the

importance of dissociating the purely hydrostatic effect from the fluid sorption over an extended pressure range.

Taking advantage of the differential mounting of the high pressure calorimetric detector and the proper use of the thermodynamic Maxwell's relation $\left(\partial S / \partial P\right)_T = -\left(\partial V / \partial T\right)_P$, a practical expression of the global cubic expansion coefficient $\alpha_{pol\text{-}g\text{-}int}$ of the saturated polymer subjected to the compressed penetrating (permeant) solvent under isothermal conditions has been established as follows by **eq. (7)**:

$$\alpha_{pol-g-\mathrm{int}} = \frac{\left(Q_{diff,SS} - Q_{diff,pol}\right) + V_{SS,r}\,\alpha_{SS}\,T\,\Delta P}{V_{pol}\,T\,\Delta P} \tag{7}$$

α_{SS} is the cubic expansion coefficient of the stainless steel of which are made the cells. V_{pol} and V_{SS} are the volumes of the polymer sample placed in the measuring cell and of the stainless steel (reference) sample placed in the reference cell, respectively. The stainless steel sample is identical in volume to the initial polymer sample. $Q_{diff,\,pol}$ is the differential heat between the measuring cell and the reference cell. $Q_{diff,\,SS}$ is the measure of the thermodynamic asymmetry of the cells. ΔP is the variation of gas-pressure during a scan at constant temperature T.

Three quite different pressure transmitting fluids, as regards their impact on a given polymer, have been selected: *i)* mercury (Hg), inert fluid, with well-established thermo-mechanical coefficients inducing exclusively hydrostatic effect, *ii)* a non-polar medium nitrogen (N_2) qualified as "poor" solvent, and *iii)* "chemically active" carbon dioxide (CO_2) (Glasser, 2002; Nalawade et al., 2006). While maintaining the temperature constant, the independent thermodynamic variables P or V can be scanned. Optimization and reliability of the results are verified by applying fast variations of pressure (P jumps), pressure scans (P scans) and volume scans (V scans) during pressurization and depressurization. Additionally, taking advantage of the differential arrangement of the calorimetric detector the comparative behaviour of two different polymer samples subjected to exactly the same supercritical conditions can be documented. As such, three main and original conclusions for quantifying the thermo-diffuso-chemo-mechanical behaviour of two polymers, a polyvinylidene fluoride (PVDF) and a medium density polyethylene (MDPE) with similar volume fraction of amorphous phase, can be drawn. This includes the reversibility of the solvent sorption/desorption phenomena, the role of the solvent (the permeant) state, *i.e.*, gaseous or supercritical state, the direct thermodynamic comparison of two polymers in real conditions of use.

The reversibility of the sorption/desorption phenomena is well observed when experiments are performed at the thermodynamic equilibrium, *i.e.*, at low rate volume scans. The preferential polymer/solvent interaction, when solvent is becoming a supercritical fluid, is emphasized with respect to the competition between plasticization and hydrostatic pressure effects. In the vicinity of the critical point of the solvent, a minimum of the $\alpha_{pol\text{-}g\text{-}int}$ coefficient is observed. It corresponds to the domain of pressure where plasticization due to the solvent sorption is counterbalanced by the hydrostatic effect of the solvent. The significant influence of the 'active' supercritical CO_2 is illustrated by more energetic interactions with PVDF than with MDPE at pressure below 30 MPa (Boyer et al., 2009). The hetero polymer/CO_2 interactions appear stronger than the homo interactions between molecular chains. PVDF more easily dissolves CO_2 than MDPE, the solubility being favoured by the presence of polar groups C-F

in the PVDF chain (Flaconnèche et al., 2001). This easiness for CO_2 to dissolve is observed at high pressure where the parameter $\alpha_{pol\text{-}g\text{-}int}$ is smaller for highly condensed {PVDF-CO_2} systems than for less condensed {MDPE-CO_2} system (Boyer et al., 2007).
With the objective to scrutinize the complex interplay of the coupled diffusive, chemical and mechanical parameters under extreme conditions of P and T, thermodynamics plays a pivotal role. Precise experimental approaches are as crucial as numerical predictions for a complete understanding of polymer behaviour in interactions with a solvent.

3.2 Thermodynamics as a means to understand and control nanometric scale length patterns using preferential liquid-crystal polymer/solvent interactions

Thermodynamics is ideally suited to obtain specific nano-scale pattern formation, for instance 'selective decoration' of arrayed polymer structure through selected additives, by controlling simultaneously the phase diagrams of fluids and of semi-crystalline polymers.
The creation of hybrid metal-polymer composite materials, with a well-controlled structure organization at the nanometric scale, is of great practical interest (Grubbs, 2005; Hamley, 2009), notably for the new generation of microelectronic and optical devices. Inorganic nanoparticles possess unique size dependent properties, from electronic, optical to magnetic properties. Among them, noble gold nanoparticles (AuNPs) are prominent. Included into periodic structures, inorganic nanoparticles can potentially lead to new collective states stemming from precise positioning of the nanoparticles (Tapalin et al., 2009). When used as thin organic smart masks, block copolymers make ideal macromolecular templates. Especially, the unique microphase separated structure of asymmetric liquid-crystal (LC) di-block copolymer (BC), like PEO-*b*-PMA(Az), develops itself spontaneously by self assemblage to form PEO channels hexagonally packed (Tian et al., 2002; Watanabe et al., 2008). PEO_m-*b*-$PMA(Az)_n$ amphiphilic diblock copolymer consists of hydrophilic poly(ethylene oxide) (PEO) entity and hydrophobic poly(methacrylate) (PMA) entity bearing azobenzene mesogens (Az) in the side chains, where m and n denote the degrees of polymerization of PEO and of photoisomarized molecules azobenzene moieties, respectively. By varying m and n, the size of the diameters of PEO cylinders is controlled from 5 to 10 nm while the distance between the cylinders is 10 to 30 nm. Four phase transitions during BC heating are ascribed to PEO crystal melting, PMA(Az) glass transition, liquid crystal transition from the smectic C (SmC) phase to the smectic A (SmA) phase and isotropic transition (Yoshida et al., 2004). In PEO_{114}-*b*-$PMA(Az)_{46}$, the temperatures of the transitions are about 311, 339, 368 and 388 K, respectively.
As such, for creating smart and noble polymer-metal hybrids possessing a structure in the nanometric domain, three original aspects are discussed. They include the initial thermodynamic polymer/pressure medium interaction, the modulation of the surface topology concomitantly with the swelling of the solvent-modified nano-phase-separated organization, the "decorative" particles distribution modulation. All the aspects have an eco-aware issue and they are characterized through a rigorous analysis of the specific interactions taking place in LC/solvent systems.

Polymer/pressurizing fluid interactions

The isobaric temperature-controlled scanning transitiometry (*T*CST) (Grolier et al., 2004; Bessières et al., 2005) is used to investigate the phase changes via the Clapeyron's equation while the pressure is transmitted by various fluids. The enthalpy, volume and entropy

changes are quantified *versus* the (high) pressure of either Hg, CO_2, or N_2 (Yamada et al., 2007a-b). The hydrostatic effect of "more or less chemically active" solvent CO_2, or N_2 is smaller than the hydrostatic effect of mercury. The adsorbed solvent induces smaller volume changes at the isotropic transition than the mercury pressure. This results from the low compressibility of solvent (gas) molecules compared to the free volume compressibility induced in BC. A particular behaviour is observed with "chemically active" CO_2 where the quadrupole-dipole interactions favour the CO_2 sorption into the PMA(Az) matrix during the isotropic liquid transition (Kamiya et al., 1998; Vogt et al., 2003). The hydrostatic effect by CO_2 overcomes above 40 MPa with a CO_2 desorption at higher pressures explained by the large change of molecular motions at the isotropic transition upon the disruption of π-bounds with azobenzene moieties.

Modulation of the surface topology and swelling of the CO_2-modified nanometric-phase-separated organization

Supercritical carbon dioxide ($SCCO_2$) constitutes an excellent agent of microphase separation. From *ex-situ* Atomic Force Microscopy (AFM) and Transmission Electron Microscopy (TEM) analysis of the pattern organization, the fine control of the pressure together with the temperature at which the CO_2 treatment is achieved demonstrates the possibility to modulate the surface topology inversion between the copolymer phases concomitantly with the swelling of the nano-phase-separated organization. The observed phase contrast results from the coupled effect of the different elastic moduli of the two domains of the block-copolymer with chemo-diffuso phenomenology.

Remarkably, the preferential CO_2 affinity is associated with the thermodynamic state of CO_2, from liquid (9 MPa, room temperarture (r.t.)) to supercritical (9 MPa, 353 K) and then to gaseous (5 MPa, r.t.) state (Glasser, 2002). This is typically observed when annealing the copolymer for 2 hours to keep the dense periodic hexagonal honeycomb array **(Fig. 3.a-d)**. Under gaseous CO_2, the surface morphology of PEO cylinders is not significantly expanded **(Fig. 3.a-b)**. However, liquid CO_2 induces a first drastic shift at the surface with the emergence of a new surface state of PEO cylinders. This surface state inversion is attributed to domain-selective surface disorganization. PMA(Az) in the glassy smectic C (SmC) phase cannot expand. PEO cylinders dissolve favourably within liquid CO_2, with polar interactions, get molecular movement, expand preferentially perpendicularly to the surface substrate **(Fig. 3.c)**. By increasing temperature, liquid CO_2 changes to supercritical CO_2. The PMA(Az) domain is in the SmC phase and get potential molecular mobility. At this stage, the copolymer chains should be easily swelled. The easiness of $SCCO_2$ to dissolve within liquid PEO cylinders deals with a new drastic change of the surface topology where the absorbed $SCCO_2$ increases the diameter of the PEO nano-tubes **(Fig. 3.d)**.

The preferential CO_2 affinities produce porous membranes with a selective sorption in hydrophilic semicrystalline 'closed loop', *i.e.*, PEO channels (Boyer et al., 2006a). More especially, under supercritical $SCCO_2$, the PEO cylinders kept in the ordered hexagonal display exhibit the highest expansion in diameter. In the case of PEO_{114}-*b*-$PMA(Az)_{46}$, the exposure to $SCCO_2$ swells the PEO cylinders by 56 %, with arrays from 11.8 nm in diameter at r.t. to 18.4 nm in diameter at 353 K. The lattice of the PMA matrix, *i.e.*, periodic plane distance between PEO cylinders, slightly increases by 26 %, from 19.8 nm at r.t. to 24.9 nm at 353 K. This microphase separation is driven by disparity in free volumes between dissimilar segments of the polymer chain, as described from the entropic nature of the closed-loop miscibility gap (Lavery et al., 2006; Yamada et al., 2007a-b).

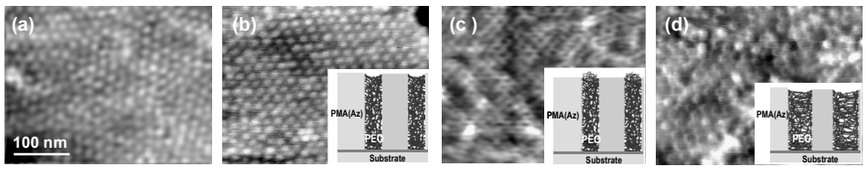

Fig. 3. Pattern control in the nanometric scale under multifaceted *T, P* and CO_2 constraints, 2 hrs annealed. AFM phase, tapping mode, illustrations on silicon substrate **(a)** neat PEO_{114}-*b*-$PMA(Az)_{46}$, PEO 'softer' than PMA(Az) appears brighter (whiter), **(b)** GCO_2 saturation (5 MPa, r.t.), **(c)** LCO_2 saturation (9 MPa, r.t.), PMA(Az) surrounding PEO becomes 'softer', **(d)** $SCCO_2$ saturation (9 MPa, 353 K), PEO becomes 'softer' while swelling. Inserts **(b-c-d)** are schematic representations of CO_2-induced changes of PEO cylinders. (BC film preparation before modification: 2 wt% toluene solution spin-coating, 2000 rpm, annealing at 423 K for 24 hrs in vacuum.)

Modulation of the decorative particles distribution

To create nano-scale hybrid of metal-polymer composites, the favourable $SCCO_2$/PEO interactions are advantageously exploited, as illustrated in **Fig. 4.a-b**. They enable a tidy pattern of hydrophilic gold nano-particles (AuNPs). AuNPs are of about 3 nm in diameter and stabilized with thiol end-functional groups (Boal & Rotello, 2000). Preferentially, the metal NPs wet one of the two copolymer domains, the PEO channels, but de-wet the other, the PMA(Az) matrix. This requires a high mobility contrast between the two copolymer domains, heightened by CO_2 plasticization that enhances the free volume disparity between copolymer parts. Each $SCCO_2$-swollen PEO hydrophilic hexagonal honeycomb allows the metal NPs to cluster. A two-dimensional (2D) periodic arrangement of hydrophilic AuNPs is generated in the organic PEO in turn confined into smectic C phase of PMA(Az) matrix which has potential molecular mobility. Additionally to the plasticizing action, the force of the trap is driving chemically. It is due to the hydrophilic compatibility of AuNPs in PEO cylinders by grafted polar groups (Watanabe et al., 2007).

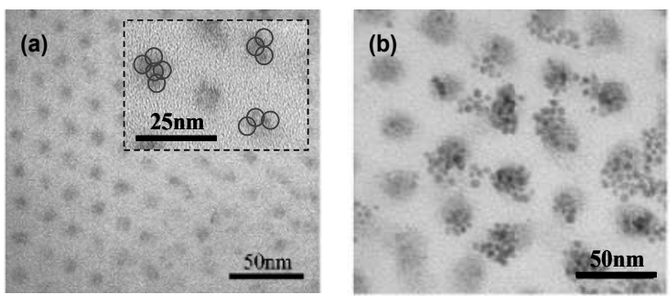

Fig. 4. Pattern control in the nanometric scale of PEO-*b*-PMA(Az) under multifaceted *T, P,* CO_2 constraints with AuNPs. TEM illustrations of BC on carbone coated copper grid **(a)** PEO_{114}-*b*-$PMA(Az)_{46}$, **(b)** PEO_{454}-*b*-$PMA(Az)_{155}$ doped with AuNPs under $SCCO_2$ (9 MPa, 353 K). Black spots are AuNPs wetted hexagonal PEO honeycomb, selectively. PEO is **(a)** 8.6, **(b)** 24.3 nm in diameter with a periodicity of **(a)** 17.1, **(b)** 36.6 nm. (Step 1, BC film preparation before modification: 2 wt% toluene solution solvent-casting, annealing at 423 K for 24 hrs in vacuum. Step 2, AuNPs deposition before modification: droplet of an ethanol solution of hydrophilic AuNPs (solvent in toluene of 1 %) on dried BC film, drying at r.t. for 2 hrs.)

The local affinities of AuNPs with PEO/$SCCO_2$ stabilize the thermodynamically unstable $SCCO_2$-plasticized network and keep it stable with time, which cannot be observed without the insertion of gold nano-particles mainly because of diffusion effect of the solvent (Boyer et al., **2006a)**. The mean height of AuNPs layer is about 3 nm, which is 20 times smaller than PEO cylinders with a 60 nm in length. Thus PEO channels could be considered as nano-dots receptors, schematically as a "compact core–shell model" consisting of a spherical or isotropic AuNP "core" embedded into a PEO channel "shell", consequently leading to isotropic two- and three-dimensional materials. Nicely, AuNPs clusters on PEO channel heads can be numerically expressed. The presence of, 4, 5 and 8 single Au nano-clusters for m = 114, 272 and 454 is identified, respectively. It represents a linear function between the number of AuNPs on swollen PEO *versus* $SCCO_2$-swollen diameter with half of ligands of AuNPs linked with PEO polymer chain.

From this understanding, a fine thermodynamic-mechanical control over extended T and P ranges would provide a precious way to produce artificial and reliable nanostructured materials. $SCCO_2$-based technology guides a differential diffusion of hydrophilic AuNPs to cluster selectively along the hydrophilic PEO scaffold. As a result, a highly organized hybrid metal-polymer composite is produced. Such understanding would be the origin of a 2D nanocrystal growth.

3.3 Thermokinetics as a means to control macrometric length scale molecular organizations through molten to solid transitions under mechanical stress

A newly developed phenomenological model for pattern formation and growth kinetics of polymers uses thermodynamic parameters, as thermo-mechanical constraints and thermal gradient. It is a system of physically-based morphological laws-taking into account the kinetics of structure formation and similarities between polymer physics and metallurgy within the framework of Avrami's assumptions.

Polymer crystallization is a coupled phenomenon. It results from the appearance (nucleation in a more or less sporadic manner) and the development (growth) of semi-crystalline entities (*e.g.*, spherulites) (Gadomski & Luczka, 2000; Panine et al., 2008). The entities grow in all available directions until they impinge on one another. The crystallization kinetics is described in an overall manner by the fraction $\alpha(t)$ (surface fraction in two dimensions (2D) or volume fraction in three dimensions (3D)) transformed into morphological entities (disks in 2D or spheres in 3D) at each time t.

The introduction of an overall kinetics law for crystallization into models for polymer processing is usually based on the Avrami-Evans's (AE) theory (Avrami, 1939, 1940, 1941; Evans, 1945). To treat non-isothermal crystallization, simplifying additional assumptions have often been used, leading to analytical expressions and allowing an easy determination of the physical parameters, *e.g.*, Ozawa (1971) and Nakamura et al. (1972) approaches. To avoid such assumptions, a trend is to consider the general AE equation, either in its initial form as introduced by Zheng & Kennedy (2004), or after mathematical transformations as presented by Haudin & Chenot (2004) and recalled here after.

General equations for quiescent crystallization

The macroscopic mechanism for the nucleation event proposed by Avrami remains the most widely used, partly because of its firm theoretical basis leading to analytical mathematical equations. In the molten state, there exist zones, the potential nuclei, from which the crystalline phase is likely to appear. They are uniformly distributed throughout the melt,

with an initial number per unit volume (or surface) N_0. N_0 is implicitly considered as constant. The potential nuclei can only disappear during the transformation according to activation or absorption ("swallowing") processes. An activated nucleus becomes a growing entity, without time lag. Conversely, a nucleus which has been absorbed cannot be activated any longer. In the case of a complex temperature history $T(t)$, the assumption of a constant number of nuclei N_0 is no more valid, because $N_0 = N_0(T) = N_0(T(t))$ may be different at each temperature. Consequently, additional potential nuclei can be created in the non-transformed volume during a cooling stage. All these processes are governed by a set of differential equations (Haudin & Chenot, 2004), differential equations seeming to be most suitable for a numerical simulation (Schneider et al., 1988).

Avrami's Equation

Avrami's theory (Avrami, 1939, 1940, 1941) expresses the transformed volume fraction $\alpha(t)$ by the general differential equation **eq. (8)**:

$$\frac{d\alpha(t)}{dt} = (1-\alpha(t))\frac{d\tilde{\alpha}(t)}{dt} \tag{8}$$

$\tilde{\alpha}(t)$ is the "extended" transformed fraction, which, for spheres growing at a radial growth rate $G(t)$, is given by **eq. (9)**:

$$\tilde{\alpha}(t) = \frac{4\pi}{3}\int_0^t \left[\int_\tau^t G(u)du\right]^3 \frac{d\tilde{N}_a(\tau)}{d\tau}d\tau \tag{9}$$

$d\tilde{N}_a(t)/dt$ is the "extended" nucleation rate, $\frac{4\pi}{3}\left[\int_\tau^t G(u)du\right]^3$ is the volume at time τ of a sphere appearing at time t, and $d\tilde{N}_a(\tau)$ are spheres created per unit volume between τ and $\tau + d\tau$.

Assumptions on Nucleation

The number of potential nuclei decreases by activation or absorption, and increases by creation in the non-transformed volume during cooling. All these processes are governed by the following equations:

$$\frac{dN(t)}{dt} = -\frac{dN_a(t)}{dt} - \frac{dN_c(t)}{dt} + \frac{dN_g(t)}{dt} \tag{10a}$$

$$\frac{dN_a(t)}{dt} = q(t)N(t) \tag{10b}$$

$$\frac{dN_c(t)}{dt} = \frac{N(t)}{1-\alpha(t)}\frac{d\alpha(t)}{dt} \tag{10c}$$

$$\frac{dN_g(t)}{dt} = (1-\alpha(t))\frac{dN_0(T)}{dT}\frac{dT}{dt} \tag{10d}$$

$N(t), N_a(t), N_c(t), N_g(t)$ are the number of potential, activated, absorbed and generated (by cooling) nuclei per unit volume (or surface) at time *t*, respectively. *q(t)* is the activation frequency of the nuclei at time *t*. The "extended" quantities $\tilde{N}, \tilde{N}_a$ are related to the actual ones by:

$$N = (1-\alpha)\tilde{N} \tag{11a}$$

$$\frac{dN_a}{dt} = qN = (1-\alpha)\frac{d\tilde{N}_a}{dt} \tag{11b}$$

The System of Differential Equations

The crystallization process equations are written into a non-linear system of six, **eqs. (12, 13a, 14-17)**, or seven, **eqs. (12, 13b, 14-18)**, differential equations in 2D or 3D conditions, respectively (Haudin & Chenot, 2004):

$$\frac{dN}{dt} = -N\left(q + \frac{1}{1-\alpha}\frac{d\alpha}{dt}\right) + (1-\alpha)\frac{dN_0(T)}{dT}\frac{dT}{dt} \tag{12}$$

$$\frac{d\alpha}{dt} = 2\pi(1-\alpha)G(F\tilde{N}_a - P) \tag{13a}$$

$$\frac{d\alpha}{dt} = 4\pi(1-\alpha)G(F^2\tilde{N}_a - 2FP + Q) \tag{13b}$$

$$\frac{dN_a}{dt} = qN \tag{14}$$

$$\frac{d\tilde{N}_a}{dt} = \frac{qN}{1-\alpha} \tag{15}$$

$$\frac{dF}{dt} = G \tag{16}$$

$$\frac{dP}{dt} = F\frac{d\tilde{N}_a}{dt} = F\frac{qN}{1-\alpha} \tag{17}$$

$$\frac{dQ}{dt} = F^2\frac{d\tilde{N}_a}{dt} = F^2\frac{qN}{1-\alpha} \tag{18}$$

The initial conditions at time *t* = 0 are:

$$N(0) = N_0$$

$$\alpha(0) = N_a(0) = \tilde{N}_a(0) = F(0) = P(0) = Q(0) = 0 \tag{19}$$

F, *P* and *Q* are three auxiliary functions added to get a first-order ordinary differential system. The model needs three physical parameters, the initial density of potential nuclei N_0,

the frequency of activation q of these nuclei and the growth rate G. In isothermal conditions, they are constant. In non-isothermal conditions, they are defined as temperature functions, *e.g.*:

$$N_0 = N_{00}\exp\left(-N_{01}(T-T_0)\right) \tag{20a}$$

$$q = q_0\exp\left(-q_1(T-T_0)\right) \tag{20b}$$

$$G = G_0\exp\left(-G_1(T-T_0)\right) \tag{20c}$$

General equations for shear-induced crystallization

Crystallization can occur in the form of spherulites, shish-kebabs, or both. The transformed volume fraction is written as (Haudin et al., 2008):

$$\frac{d\alpha(t)}{dt} = \frac{d\beta(t)}{dt} + \frac{d\kappa(t)}{dt} \tag{21}$$

$\beta(t)$ and $\kappa(t)$ are the thermo-dependent volume fractions transformed *versus* time into spherulites and into shish-kebabs, respectively.

Spherulitic Morphology

Modification of **eqs. (8)** and **(10a)** gives:

$$\frac{d\beta(t)}{dt} = (1-\alpha(t))\frac{d\tilde{\beta}(t)}{dt} \tag{22}$$

$$\frac{dN(t)}{dt} = -\frac{dN_a(t)}{dt} - \frac{dN_c(t)}{dt} + \frac{dN_g(t)}{dt} + \frac{dN_\gamma(t)}{dt} \tag{23}$$

$\beta(t)$ and $\tilde{\beta}(t)$ are the actual and extended volume fractions of spherulites, respectively. $N_\gamma(t)$ is the number of nuclei per unit volume generated by shear. Two situations are possible, *i.e.*, crystallization occurs after shear or crystallization occurs during shear.
If crystallization during shear remains negligible, the number of shear-generated nuclei is:

$$\frac{dN_\gamma}{dt} = a\dot{\gamma}(A-N_\gamma) \text{ if } a\dot{\gamma}(A-N_\gamma) \geq 0 \tag{24a}$$

$$\frac{dN_\gamma}{dt} = 0 \text{ if } a\dot{\gamma}(A-N_\gamma) \leq 0 \tag{24b}$$

a and A_1 are material parameters, eventually thermo-dependent. As a first approximation, $A = A_1\dot{\gamma}$, with $\dot{\gamma}$ the shear rate.
If crystallization proceeds during shear, only the liquid fraction is exposed to shear and the shear rate $\dot{\gamma}'$ is becoming:

$$\dot{\gamma}' = \dot{\gamma} / (1-\alpha)^{1/3} \tag{25}$$

By defining $\tilde{N}_\gamma$ as the extended number of nuclei per unit volume generated by shear in the total volume, then:

$$\frac{d\tilde{N}_\gamma}{dt} = a\dot{\gamma}'(A_1\dot{\gamma}' - \tilde{N}_\gamma) \tag{26}$$

The number N_γ of nuclei generated by shear in the liquid fraction is:

$$N_\gamma = (1-\alpha)\tilde{N}_\gamma \tag{27}$$

Under shear, the activation frequency of the nuclei increases. If the total frequency is the sum of a static component, q_{st} , function of temperature, and of a dynamic one, q_{flow} , then:

$$q = q_{st} + q_{flow} \tag{28}$$

q_{flow} is given by **eq. (29)** where as a first approximation $q_2 = q_{02}\dot{\gamma}$ and q_3 is constant.

$$q_{flow} = q_2(1 - \exp(-q_3\dot{\gamma})) \tag{29}$$

The system of differential equations **(12, 13b, 14-18)** is finally replaced by a system taking the influence of shear into account through the additional unknown N_γ and through the dynamic component of the activation frequency q_{flow}. Two cases are considered, *i.e.*, crystallization occurs after shear **(37a)** or crystallization occurs under **(37b)** shear.

$$\frac{dN}{dt} = -N\left(q + \frac{1}{1-\alpha}\frac{d\alpha}{dt}\right) + (1-\alpha)\frac{dN_0(T)}{dT}\frac{dT}{dt} + \frac{dN_\gamma}{dt} \tag{30}$$

$$\frac{d\beta}{dt} = 4\pi(1-\alpha)G(F^2\tilde{N}_a - 2FP + Q) \tag{31}$$

$$\frac{dN_a}{dt} = qN \tag{32}$$

$$\frac{d\tilde{N}_a}{dt} = \frac{qN}{1-\alpha} \tag{33}$$

$$\frac{dF}{dt} = G \tag{34}$$

$$\frac{dP}{dt} = F\frac{d\tilde{N}_a}{dt} = F\frac{qN}{1-\alpha} \tag{35}$$

$$\frac{dQ}{dt} = F^2\frac{d\tilde{N}_a}{dt} = F^2\frac{qN}{1-\alpha} \tag{36}$$

$$\frac{dN_\gamma}{dt} = a\dot{\gamma}(A_1\dot{\gamma} - N_\gamma) \tag{37a}$$

$$\frac{dN_\gamma}{dt} = a\dot{\gamma}\left((1-\alpha)^{1/3} A_1\dot{\gamma} - \frac{N_\gamma}{(1-\alpha)^{1/3}}\right) - \frac{N_\gamma}{1-\alpha}\frac{d\alpha}{dt} \tag{37b}$$

The initial conditions at time $t = 0$ are:

$$\begin{gathered} N(0) = N_0 \\ \alpha(0) = N_a(0) = \tilde{N}_a(0) = F(0) = P(0) = Q(0) = 0 \\ N_\gamma(0) = 0 \end{gathered} \tag{38}$$

Shish-Kebab Morphology

Firstly are introduced the notions of real and extended transformed volume fractions of shish-kebab, κ and $\tilde{\kappa}$, respectively. Both are related by **eq. (39)**:

$$\frac{d\kappa(t)}{dt} = (1-\alpha)\frac{d\tilde{\kappa}(t)}{dt} \tag{39}$$

$\alpha(t)$ is the total transformed volume fraction for both spherulitic and oriented phases.
Shish-kebabs are modelled as cylinders with an infinite length. The growth rate H is deduced from the radius evolution of the cylinder. The general balance of the number of nuclei for the oriented structure is given as:

$$\frac{dM(t)}{dt} = -\frac{dM_a(t)}{dt} - \frac{dM_c(t)}{dt} + \frac{dM_\gamma(t)}{dt} \tag{40}$$

$M(t)$, $M_a(t)$, $M_c(t)$, $M_\gamma(t)$ are the numbers of potential, activated, absorbed and generated (by shear) nuclei per unit volume, respectively. In the same way as for the spherulitic morphology, a set of differential equations can be defined where w is the activation frequency of the nuclei, b and B_1 the material parameters:

$$\begin{aligned} \frac{dM}{dt} &= -M\left(w + \frac{1}{1-\alpha}\frac{d\alpha}{dt}\right) \\ &+ b\dot{\gamma}\left((1-\alpha)^{1/3} B_1\dot{\gamma} - \frac{M}{(1-\alpha)^{1/3}}\right) - \frac{M}{1-\alpha}\frac{d\alpha}{dt} \end{aligned} \tag{41}$$

$$\frac{d\kappa}{dt} = 2\pi(1-\alpha)H(R\tilde{M}_a - S) \tag{42}$$

$$\frac{dM_a}{dt} = wM \tag{43}$$

$$\frac{d\tilde{M}_a}{dt} = \frac{wM}{1-\alpha} \tag{44}$$

$$\frac{dR}{dt} = H \tag{45}$$

$$\frac{dS}{dt} = R\frac{d\tilde{M}_a}{dt} = R\frac{wM}{1-\alpha} \tag{46}$$

F, *P*, *Q*, *R* and *S* are five auxiliary functions giving a first-order ordinary differential system. The initial conditions at time $t = 0$ are:

$$M(0) = M_0$$

$$\kappa(0) = M_a(0) = \tilde{M}_a(0) = R(0) = S(0) = 0 \tag{47}$$

Inverse resolution method for a system of differential equations

The crystallization, and especially the nucleation stage, is by nature a statistical phenomenon with large discrepancies between the sets of experimental data. The analytical extraction of the relevant crystallization parameters must be then considered as a multi-criteria optimization problem. As such the Genetic Algorithm Inverse Method is considered.
The Genetic Algorithm Inverse Method is a stochastic optimization method inspired from the Darwin theory of nature survival (Paszkowicz, 2009). In the present work, the Genetic Algorithm developed by Carroll (Carroll, "FORTRAN Genetic Algorithm Front-End Driver Code", site: *http://cuaerospace.com/ga*) is used (Smirnova et al., 2007; Haudin et al., 2008). The vector of solutions is represented by a parameter *Z*. In quiescent crystallization **(eqs. 20a-c)**, $Z = [N_{00}, N_{01}, q_0, q_1, G_0, G_1]$ with N_{00}, N_{01}, q_0, q_1, G_0, G_1 the parameters of non-isothermal crystallization for a spherulitic morphology. In shear-induced crystallization, $Z = [N_{00}, N_{01}, q_0, q_1, q_{02}, q_3, G_0, G_1, M_0, w, H, A_1, a, B_1, b]$ with (q_{02}, q_3, A_1, a) the parameters of shear-induced crystallization for a spherulitic morphology **(eqs. 26,29)** and (M_0, w, H, B_1, b) the parameters of shear-induced crystallization for an oriented, like shish-kebab, morphology **(eqs. 41,43,45,47)**.
The optimization is applied to the experimental evolution of the overall kinetics coupled with one kinetic parameter at a lower scale, the number of entities (density of nucleation $N_a(t)$). The system of differential equations is solved separately for each experimental set and gives the evolutions of $\alpha(t)$ and of the nuclei density defining a corresponding data file. The optimization function Q_{total} is expressed as the sum of the mean square errors of the transformed volume fraction Q_α and of the number of entities Q_{Na}.

Model-experiment-optimization confrontation

The structure development parameters are identifiable by using the optical properties of the crystallizing entities. The experimental investigations and their analysis are done thanks to crossed-polarized optical microscopy (POM) (Magill, 1962, 1962, 2001) coupled with optically transparent hot stages, a home-made sliding plate shearing device and a rotating parallel plate shearing device (*e.g.*, Linkam). Data accessible directly are: *i)* the evolution of the transformed fraction $\alpha(t)$, and the number of activated nuclei $Na(t)$, *ii)* the approximate values of the initial number of potential nuclei $N_0(T)$, activation frequency $q(T)$, and growth rate $G(T)$ for isothermal conditions and their functions of temperature for non-isothermal

conditions **(eqs. 20a-c)**. The exponential temperature evolution of the three key parameters N_0, q, G is possibly calculated from the values of the physical parameters obtained in three different ways: firstly, an approximate physical analysis with direct determination from the experiments *(APA)*, secondly, the use of the Genetic Algorithm method for an optimization based on several experiments (at least 5) done with the same specimen, thirdly, an optimization based on several experiments (at least 8) involving different polymer samples for which an important dispersion of the number of nuclei is observed (Haudin et al., 2008, Boyer et al., 2009). These sets of optimized temperature functions made it possible to validate the mathematical model in the 2D version, as illustrated in **Fig. 5.a-b-inserts**. The selected polymer is a polypropylene that is considered as a 'model material' because of its aptitude to crystallize with well-defined spherulitic entities in quiescent conditions.

Shear-induced crystallization, with a spherulitic morphology, gives access to the function $\mathrm{d}N_\gamma/\mathrm{dt}$ (N_γ is the number of nuclei per unit volume generated by shear **(eq. 23)**) *versus* time and to the shear dependence of the activation frequency for different relatively low shear rates (up to 20 s^{-1}). A set of seven optimized parameters are identifiable: N_{00}, q_0, G_0 from quiescent isothermal crystallization, and (q_{02}, q_3, A_1, a) from isothermal shear-induced crystallization. The agreement between experiment and theory is better for higher shear rates associated with a shorter total time of crystallization. The mean square error does not exceed 12 %, the average mean square error for 5 s^{-1} is equal to 6.7 %. The agreement between experiment and theory is less satisfactory for the number of spherulites, the mean square error reaches 25 %. Then, the new model is able to predict the overall crystallization kinetics under low shear with enough accuracy, when the entities are spherulitic.

Shear-induced crystallization, with both a spherulitic and an oriented morphology, is a different task. High shear rates (from 75 s^{-1}) enhance all the kinetics (nucleation, growth, overall kinetics) and lead to the formation of micron-size fibrillar (thread-like) structures immediately after shear, followed by the appearance of unoriented spherulitic structures at the later stages **(Fig. 6insert)**. The determination of the parameters for this double crystallization becomes a complicated task for a twofold reason: the quantitative data for both oriented and spherulitic structures are not available at high shear rate, and the double crystallization kinetics model requires to additionally determine the four parameters (w, H, B_1, b). So, optimization is based only on the evolution of the total transformed volume fraction **(eq. 21)**. Parameters characterizing quiescent crystallization (N_{00}, q_0, G_0) and shear-induced crystallization with the spherulitic morphology (q_{02}, q_3, A_1, a) are taken from the previous 'smooth' analysis, so that four parameters (w, H, B_1, b) characterizing the oriented structure have to be optimized.

Fig. 6. gathers the experimental and theoretical variations of the total transformed volume fraction for different shear rates. At the beginning, the experimental overall kinetics is faster than the calculated one most probably because the influence of shear rate on the activation frequency of the oriented structure is not taken into account. Since with higher shear rate thinner samples (~30 μm at 150 s^{-1}) are used, and since numerically the growth of entities is considered as three dimensional, the condition of 3D experiment seems not perfectly respected and the experiments give a slower evolution at the end. The mean square errors between numerical and experimental evolutions of the total transformed volume fraction do not exceed 19%.

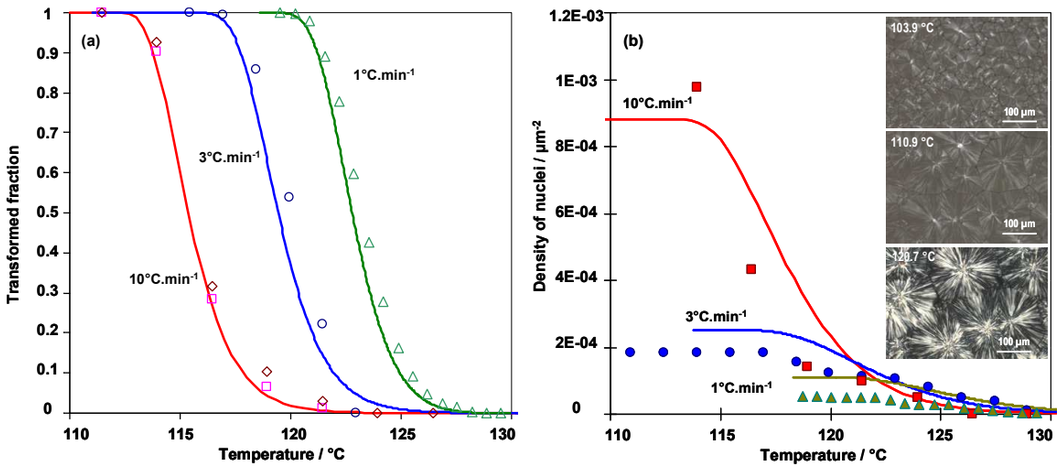

Fig. 5. Experimental (symbols) and numerically predicted (lines) of **(a)** the overall kinetics and **(b)** the number of activated nuclei *vs.* temperature at constant cooling-rate. The inserts illustrate the events at 10, 3 and 1 °C.min^{-1}. Sample: iPP in 2D (5 µm-thick layer).

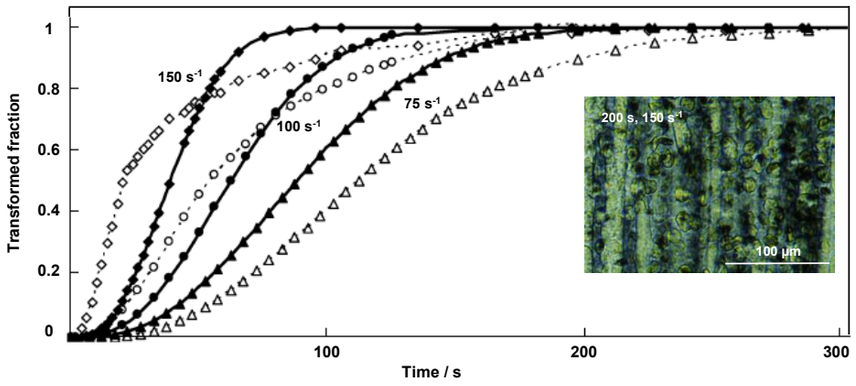

Fig. 6. Experimental (dashed-line curves) and numerically predicted (solid curves) total overall kinetics, *i.e.*, spherulitic and oriented structures, *vs.* time in constant shear, T = 132 °C. The insert illustrates the event at 150 s^{-1}. Sample: iPP in 2-3D (~30 µm-thick layer).

The present differential system, based on the nucleation and growth phenomena of polymer crystallization, is adopted to describe the crystalline morphology evolution *versus* thermo-mechanical constraints. It has been implemented into a 3D injection-moulding software. The implementation allows us to estimate its feasibility in complex forming conditions, *i.e.*, anisothermal flow-induced crystallization, and to test the sensitivity to the accuracy of the values of the parameters determined by the Genetic Algorithm Inverse Method.

4. Conclusion

Fundamental understanding of the inherent links between multiscale polymer pattern and polymer behaviour/performance is firmly anchored on rigorous thermodynamics and

thermokinetics explicitly applied over extended temperature and pressure ranges, particularly under hydrostatic stress generated by pressure transmitting fluids of different physico-chemical nature.
Clearly, such an approach rests not only on the conjunction of pertinent coupled experimental techniques and of robust theoretical models, but also on the consistency and optimization of experimental and calculation procedures.
Illustration is made with selected examples like molten and solid polymers in interaction with various light molecular weight solvents, essentially gases. Data obtained allow evaluating specific thermal, chemical, mechanical behaviours coupled with sorption effect during solid to melt as well as crystallization transitions, creating smart and noble hybrid metal-polymer composites and re-visiting kinetic models taking into account similarities between polymer and metal transformations.
This work generates a solid platform for polymer science, addressing formulation, processing, long-term utilization of end-products with specific performances controlled via a clear conception of greatly different size scales, altogether with an environmental aware respect.

5. Acknowledgments

The principal author, Séverine A.E. Boyer, wishes to address her grateful acknowledgments for financial supports from Centre National de la Recherche Scientifique CNRS (France) ; Institut Français du Pétrole IFP (France) with Mrs. Marie-Hélène Klopffer and Mr. Joseph Martin ; Core Research for Evolutional Science and Technology - Japan Science and Technology Agency CREST-JST (Japan) with Prof. Tomokazu Iyoda (Tokyo Institute of Technology TIT, Japan) ; ARMINES-CARNOT-MINES ParisTech (France) ; Conseil Régional de Provence-Alpes-Côte d'Azur and Conseil Général des Alpes-Maritimes (France) for support in the development of «CRISTAPRESS» project.
Séverine A.E. Boyer wishes to expresses her acknowledgements to Intech for selectionning the current research that has been recognized as valuable and relevant to the given theme.

6. References

Ahzi, S.; Parks, D.M.; Argon, A.S. (1991). Modeling of deformation textures evolution in semi-crystalline polymers. *Textures and Microstructures,* Vol.14-18, No1, (January 1991), pp. 1141-1146, ISSN 1687-5397(print) 1687-5400(web); doi: 10.1155/TSM.14-18.1141

Arruda, E.M.; Boyce, M.C. (1993). A three-dimensional constitutive model for the large stretch behaviour of rubber elastic materials. *Journal of the Mechanics and Physics of Solids,* Vol.41, No2, (February 1993), pp. 389-412, ISSN 0022-509; doi: 10.1016/0022.5096(93)900 13-6

Asta, M.; Beckermann, C.; Karma, A.; Kurz, W.; Napolitano, R.; Plapp, M.; Purdy, G.; Rappaz, M.; Trivedi, R. (2009). Solidification microstructures and solid-state parallels: Recent developments, future directions. *Acta Materialia*, Vol.57, No4, (February 2009), pp. 941-971; ISSN 1359-6454; doi: 10.1016/j.actamat.2008.10.020

Avrami, M. (1939). Kinetics of phase change. I General theory. *Journal of Chemical Physics,* Vol.7, No12, (December 1939), pp. 1103-1112, ISSN 0021-9606(print) 1089-7690(web); doi: 10.1063/1.1750380

Avrami, M. (1940). Kinetics of phase change. II Transformation-time relations for random distribution of nuclei. *Journal of Chemical Physics,* Vol.8, No2, (February 1940), pp. 212-224, ISSN 0021-9606(print) 1089-7690(web); doi: 10.1063/1.1750631

Avrami, M. (1941). Granulation, phase change, and microstructure. Kinetics of phase change. III. *Journal of Chemical Physics,* Vol.9, No2, (February 1941), pp. 177-184, ISSN 0021-9606(print) 1089-7690(web); doi: 10.1063/1.1750872

Baert, J.; Van Puyvelde, P.; Langouche, F.; (2006). Flow-induced crystallization of PB-1: From the low shear rate region up to processing rates. *Macromolecules,* Vol.39, No26, (November 2006), pp. 9215-9222, ISSN 0024-9297(print) 1520-5835(web); doi: 10.1021/ma062068q

Baudet, C.; Grandidier, J.-C.; Cangémi, L. (2009). A two-phase model for the diffuse-mechanical behaviour of semicrystalline polymers in gaseous environment. *International Journal of Solids and Structures,* Vol.46, No6, (March 2009), pp. 1389-1401, ISSN 0020-7683; doi: 10.1016/j.ijsolstr.2008.11.010

Bedoui, F.; Diani, J.; Régnier, G.; Seiler, W. (2006). Micromechanical modelling of isotropic elastic behaviour of semicrystalline polymers. *Acta Materialia,* Vol.54, No6, (April 2006), pp. 1513-1523, ISSN 1359-6454; doi: 10.1016/j.actamat.2005.11.028

Behme, S.; Sadowski, G.; Arlt, W. (1999). Modeling of the separation of polydisperse polymer systems by compressed gases. *Fluid Phase Equilibria,* Vol.158-160, (June 1999), pp. 869-877, ISSN 0378-3812; doi: 10.1016/S0378-3812(99)00055-2

Beret, S.; Prausnitz, J.M. (1975). Perturbed hard-chain theory: An equation of state for fluids containing small or large molecules. AIChe Journal, Vol.21, No6, (November 1975), pp. 1123-1132, ISSN 0001-1541(print) 1547-5905(web); doi: 10.1002/aic.690210612

Bessières, D.; Lafitte, Th.; Daridon, J.-L.; Randzio, S.L. (2005). High pressure thermal expansion of gases: measurements and calibration. *Thermochimica Acta,* Vol.428, No1-2, (April 2005), pp. 25-30, ISSN 0040-6031; doi: 10.1016/j.tca.2004.09.020

Binsbergen, F.L. (1973). Heterogeneous nucleation in the crystallization of polyolefins. III. Theory and mechanism. *Journal of Polymer Science: Polymer Physics Edition,* Vol.11, No1, (January 1973), pp. 117-135, ISSN 0098-1273(print) 1542-9385(web); doi: 10.1002/pol.1973.180110112

Boal, A.K.; Rotello, V.M. (2000). *Intra*- and *inter*monolayer hydrogen bonding in amide-functionalized alkanethiol self-assembled monolayers on gold nanoparticles. *Langmuir,* Vol.16, No24, (November 2000), pp. 9527-9532, ISSN 0743-7463(print) 1520-5827(web); doi: 10.1021/la0012384

Boyer, S.A.E.; Fournier, F.; Haudin, J.-M.; Gandin, Ch.-A. (2011a). Model experiments and structure development in high-pressure crystallization: the CRISTAPRESS project. *The Polymer Processing Society - 27th Annual Meeting* (Key Note), Marrakech (Maroc) May 10-14, 2011. (proceeding, 5 pages)

Boyer, S.A.E.; Ganet, P.; Robinson, P.; Melis, J.-P.; Haudin, J.-M. (2011b). Crystallization of polypropylene at high cooling rates. Microscopic and calorimetric studies. *Journal of Applied Polymer Science* – Invited conference, 4th International Conference on Polymer Behavior, International Union of Pure and Applied Chemistry (4ICPB-IUPAC), Lodz, Poland, September 20-23, 2010-, (Accepted March 2011), ISSN 0021-8995(print) 1097-4628(web)

Boyer, S.A.E.; Grolier, J.-P.E. (2005). Modification of the glass transitions of polymers by high-pressure gas solubility. *Pure and Applied Chemistry Science* – Invited conference, The 11th International Symposium on Solubility Phenomena (11th ISSP), Aveiro, Portugal, July 25-29, 2004-, Vol.77, No3, (March 2005), pp. 593-603, ISSN 0033-4545(print) 1365-3075(web); doi: 10.1351/pac200577030593

Boyer, S.A.E.; Grolier, J.-P.E.; Pison, L.; Iwamoto, C.; Yoshida, H.; Iyoda, T. (2006a). Isotropic transition behavior of an amphiphilic di-block copolymer under pressure. Carbon dioxide or mercury as pressure medium. *Journal of Thermal Analysis and Calorimetry,* Vol.85, No3, (September 2006), pp. 699-706, ISSN 1388-6150(print) 1572-8943(web); doi: 10.1007/s10973-006-7633-z

Boyer, S.A.E.; Grolier, J.-P.E.; Yoshida, H.; Haudin, J.-M.; Chenot, J.-L. (2009). Phase transitions of polymers over T and P ranges under various hydraulic fluids: Polymer/supercritical gas systems and liquid to solid polymer transitions. *Journal of Molecular Liquids* - Invited conference, Joint Conference of JMLG/EMLG Meeting 2007 and 30th Symposium on Solution Chemistry of Japan, Molecular Approaches to Complex Liquid Systems, Fukuoka, Japan, November 21-25, 2007-, Vol.147, No1-2, (July 2009), pp. 24-29, ISSN 0167-7322; doi: 10.1016/j.molliq.2009.01.016

Boyer, S.A.E.; Haudin, J.-M. (2010). Crystallization of polymers at constant and high cooling rates: A new hot stage microscopy set-up. *Polymer Testing* - Invited conference, The 45th Japanese Conference on Calorimetry and Thermal Analysis, Tokyo, Japan, September 28-30, 2009-, Vol.29, No4, (June 2010), pp. 445-452, ISSN 0142-9418; doi:10.1016/j.polymertesting.2010.02.003

Boyer, S.A.E.; Klopffer, M.-H.; Martin, J.; Grolier, J.-P.E. (2007). Supercritical gas-polymer interactions with applications in the petroleum industry. Determination of thermophysical properties. *Journal of Applied Polymer Science,* Vol.103, No3, (February 2007), pp. 1706-1722, ISSN 0021-8995(print) 1097-4628(web); doi: 10.1002/app.25085

Boyer, S.A.E.; Randzio, S.L.; Grolier, J.-P.E. (2006b). Thermal expansion of polymers submitted to supercritical CO_2 as a function of pressure. *Journal of Polymer Science Part B: Polymer Physics,* Vol.44, No1, (January 2006), pp. 185-194, ISSN 0887-6266(print) 1099-0488(web); doi: 10.1002/polb.20674

Brucato, V.; Piccarolo, S.; La Carrubba, V. (2002). An experimental methodology to study polymer crystallization under processing conditions. The influence of high cooling rates. *Chemical Engineering Science,* Vol.57, No19, (October 2002), pp. 4129-4143, ISSN 0009-2509; doi: 10.1016/S0009-2509(02)00360-3

Carroll, D.L. (2002). "FORTRAN Genetic Algorithm Front-End Driver Code", *http://cuaerospace.com/ga*.

Dahoun, A.; Canova, G.R.; Molinari, A.; Philippe, M. J.; G'Sell, C. (1991). The modelling of large strain textures and stress-strain relations of polyethylene. *Textures and Microstructures*, Vol.14-18, No1, (January 1991), pp. 347-354, ISSN 1687-5397(print) 1687-5400(web); doi: 10.1155/TSM.14-18.347

De Angelis, M.G.; Merkel, T.C.; Bondar, V.I.; Freeman, B.D.; Doghieri, F.; Sarti, G.C. (1999). Hydrocarbon and fluorocarbon solubility and dilation in poly(dimethylsiloxane): Comparison of experimental data with predictions of the Sanchez–Lacombe equation of state. *Journal of Polymer Science Part B: Polymer Physics,* Vol.37, No21, (November 1999), pp. 3011-3026, ISSN 0887-6266(print) 1099-0488(web); doi: 10.1002/(SICI)1099-0488(19991101)37:21<3011::AID-POLB11>3.0.CO;2-V

De Rosa, C.; Park, C.; Thomas, E.L.; Lotz, B. (2000). Microdomain patterns from directional eutectic solidification and epitaxy. *Nature,* Vol.405, No6785, (May 2000), pp. 433-437, ISSN 0028-0836(print) 1476-4687(web); doi: 10.1038/35013018

Devisme, S.; Haudin, J.-M.; Agassant, J.-F.; Rauline, D.; Chopinez, F. (2007). Numerical simulation of extrusion coating. Contribution to the understanding of adhesion mechanisms between grafted polypropylene and aluminium. *International Polymer Processing,* Vol.22, No1, pp. 90-104, ISSN 0930-777X

Dewimille, B.; Martin, J.; Jarrin., J. (1993). Behavior of thermoplastic polymers during explosive decompressions in a petroleum environment. *Journal de Physique. IV*, Vol. 3(2), No7, (July 1993), pp. 1559-1564, ISSN 1155-4339; doi: 10.1051/jp4:19937243

Ding, Z.; Spruiell, J.E. (1996). An experimental method for studying nonisothermal crystallization of polymers at very high cooling rates. *Journal of Polymer Science Part B: Polymer Physics*, Vol.34, No16, (September 1996), pp. 2783-2804, ISSN 0887-6266(print) 1099-0488(web); doi: 10.1002/(SICI)1099-0488(19961130) 34:16<2783::AID-POLB12>3.0.CO;2-6

Dixon, R.K. (2011). Global environment facility investments in the phase-out of ozone-depleting substances. *Mitigation and Adaptation Strategies for Global Change* (online first™ January 2011), ISSN 1381-2386(print) 1573-1596(web); doi: 10.1007/s11027-011-9281-2

Doghieri, F.; Sarti, G.C. (1996). Nonequilibrium lattice fluids: A predictive model for the solubility in glassy polymers. *Macromolecules*, Vol.29, No24, (November 1996), pp. 7885-7896, ISSN 0024-9297(print) 1520-5835(web); doi: 10.1021/ma951366c

Elmoumni, A.; Winter, H.H. (2006). Large strain requirements for shear-induced crystallization of isotactic polypropylene. *Rheologica Acta,* Vol.45, No6, (August 2006), pp. 793-801, ISSN 0035-4511(print) 1435-1528(web); doi: 10.1007/s00397-005-0082-y

Evans, U.R., (1945). The laws of expanding circles and spheres in relation to the lateral growth of surface films and the grain-size of metals. *Transactions of the Faraday Society,* Vol.41, (1945), pp. 365-374, ISSN 0014-7672; doi: 10.1039/TF9454100365

Ferreiro, V.; Douglas, J.F.; Warren, J.A.; Karim, A. (2002a). Nonequilibrium pattern formation in the crystallization of polymer blend films. *Physical review E, Statistical, nonlinear, and soft matter physics,* Vol.65, No4, (April 2002), pp. 042802 1-4, ISSN 1539-3755(print) 1550-2376(web); doi: 10.1103/PhysRevE.65.042802

Ferreiro, V.; Douglas, J.F.; Warren, J.A.; Karim, A. (2002b). Growth pulsations in symmetric dendritic crystallization in thin polymer blend films. *Physical review E, Statistical, nonlinear, and soft matter physics,* Vol.65, No5, (May 2002), pp. 051606 1-16, ISSN 1539-3755(print) 1550-2376(web); doi: 10.1103/PhysRevE.65.051606

Flaconnèche, B.; Martin, J.; Klopffer, M.-H. (2001). Permeability, diffusion, and solubility of gases in polyethylene, polyamide 11 and poy(vinylidene fluoride). *Oil & Gas Science and Technology – Rev. IFP,* Vol.56, No3, (May-June 2001), pp. 261-278, ISSN 1294-4475(print) 1953-8189(web); doi: 10.2516/ogst:2001023

Flemings, M.C. (1974). Solidification processing. *Metallurgical and Materials Transactions B,* Vol.5, No10, (October 1974), pp. 2121-2134, ISSN 1073-5615(print) 1543-1916(web); doi: 10.1007/BF02643923

Fulchiron, R.; Koscher, E.; Poutot, G.; Delaunay, D.; Régnier, G. (2001). Analysis of the pressure effect on the crystallization kinetics of polypropylene: Dilatometric measurements and thermal gradient modeling. *Journal of Macromolecular Science,*

Part B: Physics, Vol.40, No3&4, pp. 297-314, ISSN 0022-2348(print) 1525-609X(web); doi: 10.1081/MB-100106159

Gadomski, A.; Łuczka, J. (2000). On the kinetics of polymer crystallization: A possible mechanism. *Journal of Molecular Liquids*, Vol.86, No1-3, (June 2000), pp. 237-247, ISSN 0167-732; doi: 10.1016/S0167-7322(99)00145-2

Glasser, L. (2002). Equations of state and phase diagrams. *Journal of Chemical Education,* Vol.79, No7, (July 2002), pp. 874-876, ISSN 0021-9584; doi: 10.1021/ed079p874

Glasser, L. (2004). Water, water, everywhere: Phase diagrams of ordinary water substance. *Journal of Chemical Education,* Vol.81, No3, (March 2004), pp. 414-418, ISSN 0021-9584; doi: 10.1021/ed081p414

Gránásy, L.; Pusztai, T.; Warren, J.A.; Douglas, J.F.; Börzsönyi, T.; Ferreiro, V. (2003). Growth of 'dizzy dendrites' in a random field of foreign particles. *Nature Materials*, Vol.2, No2, (February 2003), pp. 92-96, ISSN 1476-1122(print) 1476-4660(web); doi: 10.1038/nmat815

Grolier, J.-P.E.; Dan, F.; Boyer, S.A.E.; Orlowska, M.; Randzio, S.L. (2004). The use of scanning transitiometry to investigate thermodynamic properties of polymeric systems over extended *T* and *p* ranges. *International Journal of Thermophysics*, Vol.25, No2, (March 2004), pp. 297-319, ISSN 0195-928X(print) 1572-9567(web); doi: 10.1023/B:IJOT.0000028469.17288.de

Grubbs, R.B. (2005). Hybrid metal–polymer composites from functional block copolymers. *Journal of Polymer Science Part A: Polymer Chemistry,* Vol.43, No19, (October 2005), pp. 4323-4673, ISSN 0887-624X(print) 1099-0518(web); doi: 10.1002/pola.20946

Hamley, I.W. (2009). Ordering in thin films of block copolymers: Fundamentals to potential applications. *Progress in Polymer Science,* Vol.34, No11, (November 2009), pp. 1161-1210, ISSN 0079-6700; doi: 10.1016/j.progpolymsci.2009.06.003

Haudin, J.-M.; Chenot, J.-L. (2004). Numerical and physical modeling of polymer crystallization. Part I: Theoretical and numerical analysis. *International Polymer Processing,* Vol.19, No3, pp. 267-274, ISSN 0930-777X

Haudin, J.-M.; Smirnova, J.; Silva, L.; Monasse, B.; Chenot, J.-L. (2008). Modeling of structure development during polymer processing. *Polymer Science, Series A. Polymer Physics,* Vol.50, No5, (May 2008), pp. 538-549, ISSN 0965-545X(print) 1555-6107(web); doi: 10.1134/S0965545X08050088

Hilic, S.; Pádua, A.A.H.; Grolier, J-P.E. (2000). Simultaneous measurement of the solubility of gases in polymers and of the associated volume change. *Review of Scientific Instruments*, Vol.71, No11, (November 2000), pp. 4236-4241, ISSN 0034-6748(print) 1089-7623(web); doi: 10.1063/1.1289675

Hoffman, J.D. (1983). Regime III crystallization in melt-crystallized polymers: The variable cluster model of chain folding. *Polymer,* Vol.24, No1, (January 1983), pp. 3-26, ISSN 0032-3861; doi:10.1016/0032-3861(83)90074-5

Janeschitz-Kriegl, H. (2006). Phases of flow-induced crystallization of i-PP: How remote pieces of the puzzle appear to fit. *Macromolecules,* Vol.39, No13, (June 2006), pp. 4448-4454, ISSN 0024-9297(print) 1520-5835(web); doi: 10.1021/ma0601215

Janeschitz-Kriegl, H.; Ratajski, E.; Stadlbauer, M. (2003). Flow as an effective promotor of nucleation in polymer melts: A quantitative evaluation. *Rheologica Acta,* Vol.42, No4, (July 2003), pp. 355-364, ISSN 0035-4511(print) 1435-1528(web); doi: 10.1007/s00397-002-0247-x

Jin, L.-W.; Claborn, K.A.; Kurimoto, M.; Geday, M.A.; Maezawa, I.; Sohraby, F.; Estrada, M.; Kaminsky, W.; Kahr, B. (2003). Imaging linear birefringence and dichroism in

cerebral amyloid pathologies. *Proceedings of the National Academy of Sciences of the United States of America,* Vol.100, No26, (December 2003), pp. 15294-15298, ISSN 0027-8424(print) 1091-6490(web); doi: 10.1073/pnas.2534647100

Kamiya, Y.; Mizoguchi, K.; Terada, K.; Fujiwara, Y.; Wang, J.-S. (1998). CO_2 sorption and dilation of poly(methyl methacrylate). *Macromolecules*, Vol.31, No2, (January 1998), pp. 472-478, ISSN 0024-9297(print) 1520-5835(web); doi: 10.1021/ma970456

Keith, H.D.; Padden, Jr., F.J. (1964). Spherulitic crystallization from the melt. I. Fractionation and impurity segregation and their influence on crystalline morphology. *Journal of Applied Physics,* Vol.35, No4, (April 1964), pp. 1270-1285, ISSN 0021-8979(print) 1089-7550(web); doi:10.1063/1.1713606

Klopffer, M.-H.; Flaconnèche, B. (2001). Transport properties of gases in polymers: Bibliographic review. *Oil & Gas Science and Technology – Rev. IFP,* Vol.56, No3, (May-June 2001), pp. 223-244, ISSN 1294-4475(print) 1953-8189(web); doi: 10.2516/ogst:2001021

Kobayashi, R. (1993). Modeling and numerical simulations of dendritic crystal growth. *Physica D: Nonlinear Phenomena*, Vol.63, No3-4, (March 1993), pp. 410-423, ISSN 0167-2789; doi: 10.1016/0167-2789(93)90120-P

Krebs, M.R.H.; Bromley, E.H.C.; Rogers, S.S.; Donald, A.M. (2005). The mechanism of amyloid spherulite formation by bovine insulin. *Biophysical Journal*, Vol.88, No3, (March 2005), pp. 2013-2021, ISSN 0006-3495(print) 1542-0086(web); doi: 10.1529/biophysj.104.051896

Lacombe, R.H.; Sanchez, I.C. (1976). Statistical thermodynamics of fluid mixtures. *The Journal of Physical Chemistry C*, Vol.80, No23, (November 1976), pp. 2568-2580, ISSN 1932-7447(print) 1932-7455(web); doi: 10.1021/j100564a009

Lavery, K.A.; Sievert, J.D.; Watkins, J.J.; Russell, T.P.; Ryu, D.Y.; Kim, J.K. (2006). Influence of carbon dioxide swelling on the closed-loop phase behavior of block copolymers. *Macromolecules,* Vol.39, No19, (September 2006), pp. 6580-6583, ISSN 0024-9297(print) 1520-5835(web); doi: 10.1021/ma060329q

Lee, L.J.; Zeng, C.; Cao, X.; Han, X.; Shen, J.; Xu, G. (2005). Polymer nanocomposite foams. *Composites Science and Technology,* Vol.65, No15-16, (December 2005), pp. 2344-2363, ISSN 0266-3538; doi: 10.1016/j.compscitech.2005.06.016

Li, Y.G.; Park, C.B.; Li, H.B.; Wang, J. (2008). Measurement of the *PVT* property of PP/CO_2 solution. *Fluid Phase Equilibria*, Vol.270, No1-2, (August 2008), pp. 15-22, ISSN 0378-3812; doi 10.1016/j.fluid.2008.05.007

Lo, C.-T.; Lee, B.; Pol, V.G.; Dietz Rago, N.L.; Seifert, S.; Winans, R.E.; Thiyagarajan, P. (2007). Effect of molecular properties of block copolymers and nanoparticles on the morphology of self-assembled bulk nanocomposites. *Macromolecules,* Vol.40, No23, (October 2007), pp. 8302-8310, ISSN 0024-9297(print) 1520-5835(web); doi: 10.1021/ma070835v

Maeda, Y.; Niori, T.; Yamamoto, J.; Yokoyama, H. (2005). Effect of pressure on phase behavior of a thermotropic cubic mesogen. *Thermochimica Acta,* Vol.428, No1-2, (April 2005), pp. 57-62, ISSN 0040-6031; doi: 10.1016/j.tca.2004.09.030

Magill, J.H. (1961). Crystallization of isotactic polypropylene using a light depolarization technique. *Nature,* Vol.191, No4793, (September 1961), pp. 1092-1093, ISSN 0028-0836(print) 1476-4687(web); doi: 10.1038/1911092a0

Magill, J.H. (1962). A new technique for following rapid rates of crystallization II Isotactic polypropylene. *Polymer,* Vol.3, (April 1962), pp. 35-42, ISSN 0032-3861; doi: 10.1016/0032-3861(62)90064-2

Magill, J.H. (2001). Review Spherulites: A personal perspective. *Journal of Materials Science*, Vol.36, No13, (July 2001), pp. 3143-3164, ISSN 0022-2461(print) 1573-4803(web); doi: 10.1023/A:1017974016928

Nakamura, K.; Watanabe, T.; Katayama, K.; Amano T. (1972). Some aspects of non-isothermal crystallization of polymers. I. Relationship between crystallization temperature, crystallinity, and cooling conditions. *Journal of Applied Polymer Science,* Vol.16, No5, (May1972), pp. 1077-1091, ISSN 0021-8995(print) 1097-4628(web); doi: 10.1002/app.1972.070160503

Nalawade, S.P.; Picchioni, F.; Janssen, L.P.B.M. (2006). Supercritical carbon dioxide as a green solvent for processing polymer melts: Processing aspects and applications. *Progress in Polymer Science,* Vol.31, No1, (January 2006), pp. 19-43, ISSN 0079-6700; doi: 10.1016/j.progpolymsci.2005.08.002

Nowacki, R.; Monasse, B.; Piorkowska, E.; Galeski, A.; Haudin, J.-M. (2004). Spherulite nucleation in isotactic polypropylene based nanocomposites with montmorillonite under shear. *Polymer,* Vol.45, No14, (June 2004), pp. 4877-4892, ISSN 0032-3861; doi: 10.1016/j.polymer.2004.04.058

Ogino, Y.; Fukushima, H.; Takahashi, N.; Matsuba, G.; Nishida, K.; Kanaya, T. (2006). Crystallization of isotactic polypropylene under shear flow observed in a wide spatial scale. *Macromolecules,* Vol.39, No22, (October 2006), pp. 7617-7625, ISSN 0024-9297(print) 1520-5835(web); doi: 10.1021/ma061254t

Okerberg, B.C.; Marand, H.; Douglas, J.F. (2008). Dendritic crystallization in thin films of PEO/PMMA blends: A comparison to crystallization in small molecule liquids. *Polymer,* Vol.49, No2, (January 2008), pp. 579-587, ISSN 0032-3861; doi: 10.1016/j.polymer.2007.11.034

Orbey, H.; Bokis, C.P.; Chen, C.-C. (1998). Equation of state modeling of phase equilibrium in the low-density polyethylene process: The Sanchez−Lacombe, statistical associating fluid theory, and polymer-Soave−Redlich−Kwong equations of state. *Industrial & Engineering Chemistry Research,* Vol.37, No11, (November 1998), pp. 4481-4491, ISSN 0888-5885(print) 1520-5045(web); doi: 10.1021/ie980220+

Ozawa, T. (1971). Kinetics of non-isothermal crystallization. *Polymer,* Vol.12, No3, (March 1971), pp. 150-158, ISSN 0032-3861; doi: 10.1016/032-3861(71)90041-3

Panayiotou, C.; Sanchez, I.C. (1991). Statistical thermodynamics of associated polymer solutions. *Macromolecules*, Vol.24, No23, (November 1991), pp. 6231-6237, ISSN 0024-9297(print) 1520-5835(web); doi: 10.1021/ma00023a027

Panine, P.; Di Cola, E.; Sztucki, M.; Narayanan, T. (2008). Early stages of polymer melt crystallization. *Polymer,* Vol.49, No3, (February 2008), pp. 676-680, ISSN 0032-3861; doi: 10.1016/j.polymer.2007.12.026

Park, C.; Yoon, J.; Thomas, E.L. (2003). Enabling nanotechnology with self assembled block copolymer patterns. *Polymer,* Vol.44, No22, (October 2003), pp. 6725-6760, ISSN 0032-3861; doi: 10.1016/j.polymer.2003.08.011

Paszkowicz, W. (2009). Genetic Algorithms, a nature-inspired tool: Survey of applications in materials science and related fields. *Materials and Manufacturing Processes,* Vol.24, No2, (February 2009), pp. 174-197, ISSN 1042-6914(print) 1532-2475(web); doi: 10.1080/10426910802612270

Pawlak, A.; Chapel, J.-P.; Piorkowska, E. (2002). Morphology of iPP spherulites crystallized in a temperature gradient. *Journal of Applied Polymer Science,* Vol.86, No6, (November 2002), pp. 1318-1328, ISSN 0021-8995(print) 1097-4628(web); doi: 10.1002/app.11269

Piorkowska, E.; Galeski, A.; Haudin, J.-M. (2006). Critical assessment of overall crystallization kinetics theories and predictions. *Progress in Polymer Science*, Vol.31, No6, (June 2006), pp. 549-575, ISSN 0079-6700; doi: 10.1016/j.progpolymsci.2006.05.001

Prigogine, I.; Bellemans, A.; Mathot, V. (1957). The molecular theory of solutions. *North-Holland Pub. Co. (Amsterdam) 1957. ID* 101-186-725 *(Last edited on 2002/02/27 17:06:35 US/Mountain)*

Rambert, G.; Jugla, G.; Grandidier, J.-C.; Cangémi, L. (2006). A modelling of the direct couplings between heat transfer, mass transport, chemical reactions and mechanical behaviour. Numerical implementation to explosive decompression. *Composites Part A: Applied Science and Manufacturing,* Vol.37, No4, (April 2006), pp. 571-584, ISSN 1359-835X; doi: 10.1016/j.compositesa.2005.05.021

Ratajski, E.; Janeschitz-Kriegl, H. (1996). How to determine high growth speeds in polymer crystallization. *Colloid & Polymer Science,* Vol.274, No10, (October 1996), pp. 938-951, ISSN 0303-402X(print) 1435-1536(web); doi: 10.1007/BF00656623

Rousset, Ph.A.; Rappaz, M.; Minner, E. (1998). Polymorphism and solidification kinetics of the binary system POS–SOS. *Journal of the American Oil Chemists' Society*, Vol.75, No7, (July 1998), pp. 857-864, ISSN 0003-021X(print) 1558-9331(web); doi: 10.1007/s11746-998-0237-y

Sanchez, I.C.; Lacombe, R.H. (1976). An elementary molecular theory of classical fluids. Pure fluids. *The Journal of Physical Chemistry*, Vol.80, No21, (October 1976), pp. 2352-2362, ISSN 1932-7447; doi: 10.1021/j100562a008

Sánchez, M.S.; Mathot, V.B.F.; Poel, G.V.; Gómez Ribelles, J.L. (2007). Effect of the cooling rate on the nucleation kinetics of poly(L-lactic acid) and its influence on morphology. *Macromolecules*, Vol.40, No22, (September 2007), pp. 7989-7997, ISSN 0024-9297(print) 1520-5835(web); doi: 10.1021/ma0712706

Sarti, G.C.; Doghieri, F. (1998). Predictions of the solubility of gases in glassy polymers based on the NELF model. *Chemical Engineering Science,* Vol.53, No19, (October 1998), pp. 3435-3447, ISSN 0009-2509; doi: 10.1016/S0009-2509(98)00143-2

Sato, Y.; Yurugi, M.; Fujiwara, K.; Takishima, S.; Masuoka, H. (1996). Solubilities of carbon dioxide and nitrogen in polystyrene under high temperature and pressure. *Fluid Phase Equilibria*, Vol.125, No1-2, (October 1996), pp. 129-138, ISSN 0378-3812; doi: 10.1016/S0378-3812(96)03094-4

Sato, Y.; Iketani, T.; Takishima, S.; Masuoka, H. (2000). Solubility of hydrofluorocarbon (HFC-134a, HFC-152a) and hydrochlorofluorocarbon (HCFC-142b) blowing agents in polystyrene. *Polymer Engineering & Science*, Vol.40, No6, (June 2000), pp. 1369-1375, ISSN 0032-3888(print) 1548-2634 (web); doi: 10.1002/pen.11266

Schick, C. (2009). Differential scanning calorimetry (DSC) of semicrystalline polymers. *Analytical and Bioanalytical Chemistry*, Vol.395, No6, (November 2009), pp. 1589-1611, ISSN 1618-2642(print) 1618-2650(web); doi: 10.1007/s00216-009-3169-y

Scheichl, R.; Klopffer, M.-H.; Benjelloun-Dabaghi, Z.; Flaconnèche, B. (2005). Permeation of gases in polymers: Parameter identification and nonlinear regression analysis. *Journal of Membrane Science*, Vol.254, No1-2, (June 2005), pp. 275-293, ISSN 0376-7388; doi: 10.1016/j.memsci.2005.01.019

Schneider, W.; Köppl, A.; Berger, J. (1988). Non-isothermal crystallization of polymers. System of rate equation. *International Polymer Processing*, Vol.2, No3-4, pp. 151-154, ISSN 0930-777X

Smirnova, J.; Silva, L.; Monasse, B.; Haudin, J.-M.; Chenot, J.-L. (2007). Identification of crystallization kinetics parameters by genetic algorithm in non-isothermal conditions. *Engineering Computations*, Vol.24, No5, pp. 486-513, ISSN 0264-4401; doi: 10.1108/02644400710755889

Sorrentino, A.; Pantani, R.; Picarella, D.; Titomanlio, G. (2005). A novel apparatus for solidification of polymer samples under simultaneous high pressures and high cooling rates. *Review of Scientific Instruments*, Vol.76, No8, (August 2005), pp. 083901-083905, ISSN 0034-6748(print) 1089-7623(web); doi: 10.1063/1.1986987

Talapin, D.V.; Shevchenko, E.V.; Bodnarchuk, M.I.; Ye, X.; Chen, J.; Murray, C.B. (2009). Quasicrystalline order in self-assembled binary nanoparticle superlattices. *Nature*, Vol.461, No7266, (October 2009), pp. 964-967, ISSN 0028-0836(print) 1476-4687(web); doi: 10.1038/nature08439

Tian, Y.; Watanabe, K.; Kong, X.; Abe, J.; Iyoda, T. (2002). Synthesis, nanostructures, and functionality of amphiphilic liquid crystalline block copolymers with azobenzene moieties. *Macromolecules*, Vol.35, No9, (April 2002), pp. 3739-3747, ISSN 0024-9297(print) 1520-5835(web); doi: 10.1021/ma011859j

Tomasko, D.L.; Li, H.; Liu, D.; Han, X.; Wingert, M.J.; Lee, L.J.; Koelling, K.W. (2003). A review of CO_2 applications in the processing of polymers. *Industrial & Engineering Chemistry Research*, Vol.42, No25, (December 2003), pp. 6431-6456, ISSN 0888-5885(print) 1520-5045(web); doi: 10.1021/ie030199z

Trivedi, R.; Laorchan, V. (1988a). Crystallization from an amorphous matrix-I. Morphological studies. *Acta Metallurgica Materialia*, Vol.36, No8, (August 1988), pp. 1941-1950, ISSN 0001-6160; doi: 10.1016/0001-6160(88)90296-9

Trivedi, R.; Laorchan, V. (1988b). Crystallization from an amorphous matrix-II. Growth kinetics. *Acta Metallurgica*, Vol.36, No8, (August 1988), pp. 1951-1959, ISSN 0001-6160; doi: 10.1016/0001-6160(88)90297-0

Van der Beek, M.H.E.; Peters, G.W.M.; Meijer, H.E.H. (2005). The influence of cooling rate on the specific volume of isotactic poly(propylene) at elevated pressures. *Macromolecular Materials and Engineering*, Vol.290, No5, (May 2005), pp. 443-455, ISSN 1438-7492(print) 1439-2054(web); doi: 10.1002/mame.200500027

Varma-Nair, M.; Handa, P.Y.; Mehta, A.K.; Agarwal, P. (2003). Effect of compressed CO_2 on crystallization and melting behavior of isotactic polypropylene. *Thermochimica Acta*, Vol.396, No1-2, (February 2003), pp. 57-65, ISSN 0040-6031; doi: 10.1016/S0040-6031(02)00516-6

Vieth, W.R.; Howell, J.M.; Hsieh J.H. (1976). Dual sorption theory. *Journal of Membrane Science*, Vol.1, (1976), pp. 177-220, ISSN 0376-7388; doi: 10.1016/S0376-7388(00)82267-X

Vogt, B.D.; Ramachandra Rao, V.S.; Cupta, R.R.; Lavery, K.A.; Francis, T.J.; Russell, T.P.; Watkins, J.J. (2003). Phase behavior of polystyrene-*block*-poly(*n*-alkyl methacrylate)s dilated with carbon dioxide. *Macromolecules*, Vol.36, No11, (April 2003), pp. 4029-4036, ISSN 0024-9297(print) 1520-5835(web); doi: 10.1021/ma0300544

Wang, L.; Li, Q.; Shen, C. (2010). The numerical simulation of the crystallization morphology evolution of semi-crystalline polymers in injection molding. *Polymer-Plastics Technology and Engineering*, Vol.49, No10, (August 2010), pp. 1036-1048, ISSN 0360-2559(print) 1525-6111(web); doi: 10.1080/03602559.2010.482088

Watanabe, K.; Suzuki, T.; Masubuchi, Y.; Taniguchi, T.; Takimoto, J.-I.; Koyama, K. (2003). Crystallization kinetics of polypropylene under high pressure and steady shear

flow. *Polymer*, Vol.44, No19, (September 2003), pp. 5843-5849, ISSN 0032-3861; doi: 10.1016/S0032-3861(03)00604-9

Watanabe, S.; Fujiwara, R.; Hada, M.; Okazaki, Y.; Iyoda, T. (2007). Site-specific recognition of nanophase-separated surfaces of amphiphilic block copolymers by hydrophilic and hydrophobic gold nanoparticles. *Angewandte Chemie International Edition*, Vol.46, No7, (February 2007), pp. 1120-1123, ISSN 1433-7851(print) 1521-3773(web); doi: 10.1002/anie.200603516

Watanabe, R.; Kamata, K.; Iyoda, T. (2008). Smart block copolymer masks with molecule-transport channels for total wet nanopatterning. *Journal of Materials Chemistry*, Vol.18, No45, (October 2008), pp. 5482-5491, ISSN 0959-9428(print+web) 1364-5501(web only); doi: 10.1039/B806378H

Winter, H.H.; Gappert, G.; Ito, H. (2002). Rigid pore structure from highly swollen polymer gels. *Macromolecules*, Vol.35, No9, (March 2002), pp. 3325-3327, ISSN 0024-9297(print) 1520-5835(web); doi: 10.1021/ma0119225

Wissinger, R.G.; Paulaitis, M.E. (1987). Swelling and sorption in polymer-CO_2 mixtures at elevated pressures. *Journal of Polymer Science Part B: Polymer Physics,* Vol.25, No12, (December 1987), pp. 2497-2510, ISSN 0887-6266(print) 1099-0488(web); doi: 10.1002/polb.1987.090251206

Wong, B.; Zhang, Z.; Handa, Y.P. (1998). High-precision gravimetric technique for determining the solubility and diffusivity of gases in polymers. *Journal of Polymer Science Part B: Polymer Physics*, Vol.36, No12, (September 1998), pp. 2025-2032, ISSN 0887-6266(print) 1099-0488(web); doi: 10.1002/(SICI)1099-0488(19980915)36:12<2025::AID-POLB2>3.0.CO;2-W

Yamada, T.; Boyer, S.A.E.; Iyoda, T.; Yoshida, H.; Grolier, J.-P.E. (2007a). Isotropic transition of amphiphilic side-chain type liquid crystalline di-block copolymers. Effects of nitrogen pressure. *Journal of Thermal Analysis and Calorimetry*, Vol.89, No1, (July 2007), pp. 9-12, ISSN 1388-6150(print) 1572-8943(web); doi: 10.1007/s10973-006-8451-z

Yamada, T.; Boyer, S.A.E.; Iyoda, T.; Yoshida, H.; Grolier, J.-P.E. (2007b). Effects of CO_2 pressure on isotropic transition of amphiphilic side-chain type liquid crystalline di-block copolymers. *Journal of Thermal Analysis and Calorimetry*, Vol.89, No3, (September 2007), pp. 717-721, ISSN 1388-6150(print) 1572-8943(web); doi: 10.1007/s10973-006-7960-0

Yoshida, H.; Watanabe, K.; Watanabe, R.; T. Iyoda (2004). Self assembled structure of amphiphilic di-block copolymer having azobenzene moieties. *Transactions of the Materials Research Society of Japan*. Vol.29, No3, (May 2004), pp. 861-864, ISSN 1382-3469

Zheng, R.; Kennedy, P.K. (2004). A model for post-flow induced crystallization: General equations and predictions. *Journal of Rheology,* Vol.48, No4, (July 2004), pp. 823-842, ISSN 0148-6055; doi: 10.1122/1.1763944

Zhong, C.; Masuoka, H. (1998). Modeling of gas solubilities in polymers with cubic equation of state. *Fluid phase equilibria,* Vol.144, No1-2, (February 1998), pp. 49-57, ISSN 0378-3812; doi: 10.1016/S0378-3812(97) 00243-4

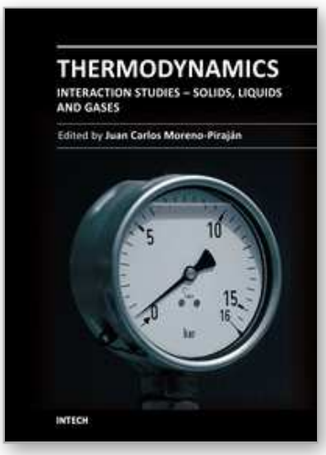

Thermodynamics - Interaction Studies - Solids, Liquids and Gases
Edited by Dr. Juan Carlos Moreno PirajÃ¡n

ISBN 978-953-307-563-1
Hard cover, 918 pages
Publisher InTech
Published online 02, November, 2011
Published in print edition November, 2011

Thermodynamics is one of the most exciting branches of physical chemistry which has greatly contributed to the modern science. Being concentrated on a wide range of applications of thermodynamics, this book gathers a series of contributions by the finest scientists in the world, gathered in an orderly manner. It can be used in post-graduate courses for students and as a reference book, as it is written in a language pleasing to the reader. It can also serve as a reference material for researchers to whom the thermodynamics is one of the area of interest.

How to reference
In order to correctly reference this scholarly work, feel free to copy and paste the following:

Séverine A.E. Boyer, Jean-Pierre E. Grolier, Hirohisa Yoshida, Jean-Marc Haudin and Jean-Loup Chenot (2011). Thermodynamics and Thermokinetics to Model Phase Transitions of Polymers over Extended Temperature and Pressure Ranges Under Various Hydrostatic Fluids, Thermodynamics - Interaction Studies - Solids, Liquids and Gases, Dr. Juan Carlos Moreno PirajÃ¡n (Ed.), ISBN: 978-953-307-563-1, InTech, Available from: http://www.intechopen.com/books/thermodynamics-interaction-studies-solids-liquids-and-gases/thermodynamics-and-thermokinetics-to-model-phase-transitions-of-polymers-over-extended-temperature-a

INTECH
open science | open minds

InTech Europe
University Campus STeP Ri
Slavka Krautzeka 83/A
51000 Rijeka, Croatia
Phone: +385 (51) 770 447
Fax: +385 (51) 686 166
www.intechopen.com

InTech China
Unit 405, Office Block, Hotel Equatorial Shanghai
No.65, Yan An Road (West), Shanghai, 200040, China
中国上海市延安西路65号上海国际贵都大饭店办公楼405单元
Phone: +86-21-62489820
Fax: +86-21-62489821

© 2011 The Author(s). Licensee IntechOpen. This is an open access article distributed under the terms of the Creative Commons Attribution 3.0 License, which permits unrestricted use, distribution, and reproduction in any medium, provided the original work is properly cited.

IntechOpen

IntechOpen